Organic LEDs for Optoelectronic Neural Networks

by

Risha R Mars

Submitted to the Department of Electrical Engineering and Computer Science
in partial fulfillment of the requirements for the degree of

Master of Engineering in Electrical Engineering and Computer Science

at the

MASSACHUSETTS INSTITUTE OF TECHNOLOGY

June 2012

Author .....
Department of Electrical Engineering and Computer Science
May 21, 2012

Certified by .....
Cardinal Warde
Professor
Thesis Supervisor

Accepted by .....
Prof. Dennis M. Freeman
Chairman, Masters of Engineering Thesis Committee

Organic LEDs for Optoelectronic Neural Networks

by

Risha R Mars

Submitted to the Department of Electrical Engineering and Computer Science
on May 21, 2012, in partial fulfillment of the
requirements for the degree of
Master of Engineering in Electrical Engineering and Computer Science

Abstract

In this thesis, I investigate the characteristics of Organic Light Emitting Diodes (OLEDs) and assess their suitability for use in the Compact Optoelectronic Integrated Neural (COIN) coprocessor. The COIN coprocessor, a prototype artificial neural network implemented in hardware, seeks to implement neural network algorithms in native optoelectronic hardware in order to do parallel type processing in a faster and more efficient manner than all-electronic implementations. The feasibility of scaling the network to tens of millions of neurons is the main reason for optoelectronics - they do not suffer from crosstalk and other problems that affect electrical wires when they are densely packed. I measured the optical and electrical characteristics different types of OLEDs, and made calculations based on existing optical equipment to determine the specific characteristics required if OLEDs were to be used in the prototype. The OLEDs were compared to Vertical Cavity Surface Emitting Lasers (VCSELs) to determine the tradeoffs in using one over the other in the prototype neural network.

Thesis Supervisor: Cardinal Warde
Title: Professor

Acknowledgments

I'd like to express my gratitude to Professor Warde for giving me the opportunity to work on this project, and for lots of interesting group meetings full of explanations and diagrams, and for his patience throughout the year. I would like to wish him success with his endeavors with the Caribbean Science Foundation, as I am sure we would both very much like to see more advancement of science and technology taking place in our homelands. I am also very grateful to Bill Herrington, for his suggestions whenever I was stuck, and his help with the optical equipment. Additionally, thanks to Sulinya Ramanan for teaching me how to make OLEDs and for providing well-made ones for experiments.

I would also like to thank my parents (Mom,Dad,Ricardo,Errolyn) for providing me with a great life and for enabling me to come to MIT and take part in a great university experience. Thanks also to all my friends, who were an integral part of this experience.

Contents

List of Figures

List of Tables

Chapter 1

Introduction

The COIN co-processor project aims to create an artificial neural network (ANN) in the hopes of advancing a different paradigm of processing. This thesis will aim to contribute to this project by outlining one approach to building a prototype Artificial Neural Network using Organic Light Emitting Diodes (OLEDs) as the emitter components. First, a brief overview of Artificial Neural Networks, the COIN co-processor project and of OLEDs would be useful.

1.1 Artificial Neural Networks

Traditional computing is done using the von Neumann architecture. This makes computers very good at doing complex mathematical problems, which require lots of calculations. However, this architecture is not suitable for processing that requires 'human' judgment, such as face recognition or learning. Humans are much better at certain classification tasks than computers, such as picking out a familiar voice in a noisy crowd, understanding speech produced from various other humans, and recognizing the faces of others even with modifications, e.g. wearing a hat, or scars. The brain's processing architecture is the neural network. It is hoped that constructing a computer with architecture similar to that of a human brain will allow the computer to 'think' like a human, and will allow the computer to perform certain processing tasks much faster.

Artificial Neural Networks (ANNs) are traditionally used for pattern recognition and classification computing tasks [9]. They are usually modeled by a set of nodes (grouped into layers) and weighted interconnections. The nodes model biological neurons, the connections model synapses, and the weights on the connections between layers model different synapse strengths [9]. The ANN has an input layer, where information is given to the system, an output layer, where the results of the computation are presented, and a varying number of intermediate or 'hidden' layers, which do the processing (see Figure 1-1).

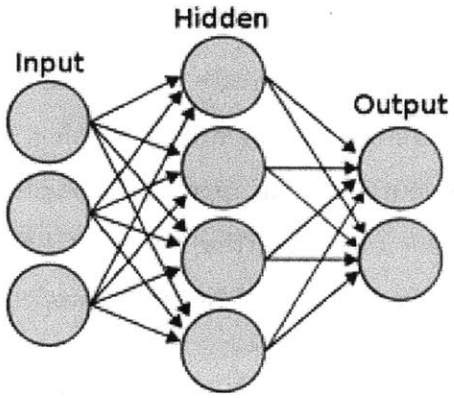

Figure 1-1: Basic model of an Artificial Neural Network [3]

Information is transmitted (and processing is accomplished) in the network by propagating signals through the layers of neurons. Each layer has detectors and emitters. The detectors in a layer receive signals from the previous layer, the layer does some processing, and then sends some signal to the next layer via the emitter. This is akin to neurons in that layer receiving a signal, then firing, propagating the signal to the next layer. Different interconnections can have different weights and so affect the signal that arrives at a particular layer (since signals arriving from different interconnections would have different strengths) [8]. When a neuron receives a signal, whether it in turn fires depends on an activation function (also called thresholding function).

Figure 1-2 shows a mathematical model of a neuron, with inputs x_i. Each synapse

has weight w_i. The output of this neuron is modeled by equation 1.1 from [22]:

$$y = f\{\sum_{i=1}^{k} x_i w_i\} \tag{1.1}$$

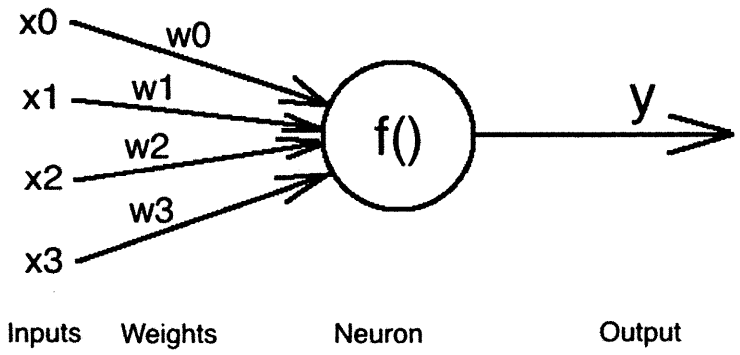

Figure 1-2: Basic model of an neuron, showing inputs and output [22]

Signals can propagate through the network without cycling back to previous layers - this is a feed-forward network. ANNs that have cycles (feedback) are called recursive or recurrent neural networks. Note that if one only has one available intermediate layer, one can simulate having multiple layers by feeding the output from that layer back into its input. This is still a feed-forward network. In this thesis, I will consider one type of feedforward implementation, a Multilayer Perceptron (MLP) network.

Like the human brain, an ANN must learn to do a particular task before it can accomplish this task - we make the ANN 'learn' a particular task by training it using a training algorithm with a particular set of data. The most commonly used training algorithm is the back propagation (BP) algorithm. With this algorithm, an input and a desired output is presented to the system. The system adjusts the weights on each layer, reducing the error between the actual and desired output until a desired error threshold is reached [22]. However, the BP algorithm is not suitable

for training a hardware implementation of an ANN, and so another algorithm, the weight perturbation (WP) algorithm, is used. WP changes the weights of the system and measures the output, as opposed to BP, which calculates the outputs based on the activation function.

1.2 Physical Implementation of Optical Neural Networks

One can write programs to simulate neural networks, but significant gains in speed can be made if the neural network is implemented in the hardware [22, 23]. If the algorithms are implemented in software, the time taken for this recall is simply too slow for the demands of the system. Thus, a system where each neuron does a small amount of on-chip computation is better - the neural network then does all its processing in parallel, which is much faster for the types of problems we want to solve [12]. The two important considerations when trying to implement a large-scale neural network prototype are the connections between neurons and the precision required to connect the synapses [11].

In the artificial neural network previously implemented in Prof. Warde's lab, the signals fired by the neurons are modeled with light beams from lasers, while the receptors in each layer are modeled by photodetectors [22]. It has been theorized that OLEDs would be a better choice for the emitters in the model than VCSELs, because of their lower cost, lower power consumption, and more compact size than the typical VCSEL. The small size of the neural network and the nature of the signal propagation require light transmission between each layer to be accurately directed. This can be accomplished by using LEDs with highly directional output.

1.2.1 Motivation for Optoelectronics

There is a need to develop a fast and compact processing system if processing of this kind is to be made commercial [26] . Optoelectronics have several advantages

over traditional electronic components. Optical components do not suffer from cross talk like traditional electric components. For multidimensional processing, such as machine vision and pattern recognition, optoelectronics are faster [26].

One difficulty in constructing a neural network prototype is the necessity of connecting each layer [22]. Neural networks are difficult to implement with traditional electronics for this very reason. VLSI systems have a flat layout, and few places where output can be taken from one chip and input to another (even though intra chip communication is good). This makes a high degree of connectivity hard to achieve [11]. Using optoelectronics is more suitable this process, though some work is required to guide light from one layer to another.

VLSI systems also consume a lot of power and are expensive to build on the required scale [11]. Delay in signal propagation through these systems is yet another reason to favor a solution which does not require traditional electronic solutions - light communications travel faster than electrical communications, and does not suffer from the crosstalk problems of electronic wires, given the high degree of connectivity required.

Adding optical emitters and photodetectors to the VLSI chip go far in solving the problems mentioned. One can now send more signals per chip using a smaller area, increasing the number of connections between chips, and propagating signals faster [11].

1.3 Compact Optoelectronic Integrated Neural (COIN) Coprocessor

The COIN coprocessor is a rough physical prototype artificial neural network setup, designed to run neural network algorithms natively on hardware which consists of optoelectronics, optical interconnects and VLSI circuits[21]. It is reconfigurable, so that the network can be easily trained on different inputs.

In its original design, the COIN coprocessor consisted of layers of neurons con-

nected by efficient holographic interconnections. The repeating structure in the design was a layer of photodetectors, followed (in order) by thresholding electronics, an array of VCSELs, a Bragg diffraction grating, and a spacing plate. The photodetector array detect incoming optical signals. The thresholding electronics determined whether the neuron would fire based on the input detected by the photodetector array. If it was determined that the neuron would fire, a VCSEL was powered. Light from the VCSEL then travelled to the next layer (guided appropriately by the Bragg grating). In reality, only one layer (containing all these components) was made, and multiple layers were simulated by feeding the output of this layer through a computer, back into itself as if it were the next layer. The neurons were connected in a nearest neighbor fashion, as shown in Figure 1-3 where one pixel in one layer would be connected (optically) to 9 pixels in the next layer [21, 22].

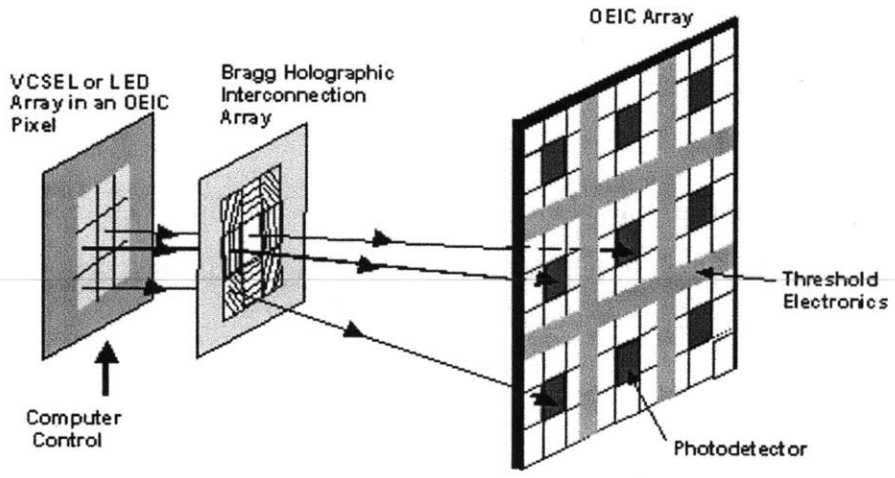

Figure 1-3: Diagram from the COIN coprocessor prototype showing nearest neighbor connections (from [21])

Weights in the neurons were simulated by varying the intensity of the light emitted from the VCSEL. The holograms needed to be highly efficient, as a lot of the power in the network would be lost through them. VLSI circuitry was employed to do the thresholding. The required weights would be stored digitally, and used to modify the laser light emitted.

The first COIN prototype was a simulated multi-layer perceptron $12 \times 12 \times 5$

network [21]. The prototype was trained using a MATLAB simulation to save time (as it would take longer to train it on the physical prototype as it was). The network was able to successfully complete training and distinguished three 12×12 pixel grayscale images presented to it.

While this initial prototype was successful, there are several areas in which it could be improved. New training algorithms could be implemented. The training weights could be stored in the layers instead of externally to improve processing time. The different components of the prototype (VCSEL lasers, holographic interconnections, VLSI thresholding) could all be improved by using different components entirely, or by optimizing their design.

1.3.1 VCSELs as light emitters in the COIN Coprocessor

Vertical Cavity Surface Emitting Lasers (VCSELs) are lasers which emit light perpendicular to the surface of the semiconductor device (as opposed to emitting light out through the edges, which is how lasers operate traditionally). The properties obtained from VCSELs have been greatly improved over the years as they become important for optical communications applications - operating powers and currents are typically less than 1.8 V and 10mA to give 1 mW or more of power [13]. Wall-plug efficiencies (ratio of output optical power to input electrical power) of up to 28% have been shown in [13], and more modern VCSELs commercially available today can have as much as 45% efficiency [17].

Vertical Cavity Surface Emitting Lasers (VCSELs) were chosen for the prototype COIN Coprocessor in [22]. They were chosen because of their narrow beam size (and low divergence) which allowed easy manipulation of the light. The high optical power obtained from the VCSELs were also advantageous, and the VCSELs worked well with the holographic interconnections used [22].

1.4 Motivation for OLEDs over VCSELs in the COIN coprocessor

While VCSELs offered several advantages when building the prototype in [22], the use of OLEDs could prove quite beneficial. OLEDs can be readily made in the laboratory in a number of customizable configurations. They do not consume much power, nor do they take up space, and can be made in very small sizes. Their properties can be easily altered, and several types of OLEDs can be investigated for use.

VCSELs are fairly expensive to manufacture, as the hybrid silicon/gallium arsenide materials from which they are made tend to be costly. OLED organic materials are cheaper to obtain, although it should be noted that significantly better properties are obtained from OLEDs made with state of the art materials and techniques, which are more expensive.

1.5 Outline of work to be presented in this thesis

This thesis will focus on the design and characterization of a section of the prototype artificial neural network. Specifically, it will discuss the optical emitter components in the prototype design - the OLEDs. The optical and electrical characteristics of OLEDs (both from the laboratory and from latest research in the field) will be investigated. The characteristics found will be compared against the presently used VCSELs to determine the suitability of OLEDs for use in the COIN coprocessor. Also discussed in this thesis is methods of how the OLEDs will fit with components around them (the input and output interfaces to the OLEDs).

Chapter 1 discussed artificial neural networks and the state of the current COIN coprocessor prototype. Chapter 2 will give an introduction to OLED devices, and considerations concerning them. Chapter 3 describes the experiments undertaken and presents the results of those experiments. Chapter 4 describes the components designed for the system. Chapter 5 shows how the findings from the experiments conducted relate to the prototype design. Finally, Chapter 6 summarizes the findings

and suggests areas for further advancement of the project.

Chapter 2

Organic Light Emitting Diodes (OLEDs)

2.1 Structure and Principle of Operation of OLEDs

An OLED operates on basically the same principles as a regular Light Emitting Diode (LED). Essentially, current is passed through an emissive layer and the recombination of holes and electrons in this region produces light. The wavelength of the light depends on the properties (specifically, bandgap) of the material used in the active layer. In a regular LED, this emissive layer is a semiconductor such as silicon or germanium. In OLEDs, this layer is made of (organic) polymer.

The basic structure of an OLED is shown in Figure 2-1 (from [7]). The OLED is made by placing a material onto a substrate which supports the structure (usually glass, but can also be flexible plastic polymer). Current is supplied via a cathode (which provides electrons) and a transparent anode (which provides holes) to the active region. Between the anode and cathode lie two or three organic layers. The conducting layer assists in carrier mobility, transporting holes from the anode. The emissive layer is made up of a different material from the conductive layer. It is where the holes and electrons recombine to emit light. Note that, like an inorganic LED, there is a hole transport layer (HTL) and an electron transport layer (ETL). The ETL and the emissive layer can be combined.

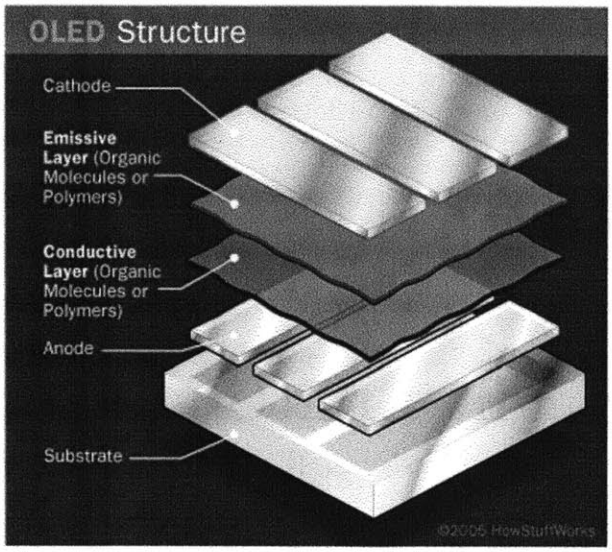

Figure 2-1: Diagram showing OLED structure [7]

A photo of one of the OLEDs made during thesis work is shown in Figure 2-2. The substrate here is a glass square. 10 individually controllable OLED devices are on the substrate (circled in Figure 2-2). For most of the testing discussed in Chapter 3, only 6 of these devices are powered and lit. Figure 2-3a in Section 2.3 shows a glass square with 6 lit OLEDs, where the individual devices can be clearly distinguished.

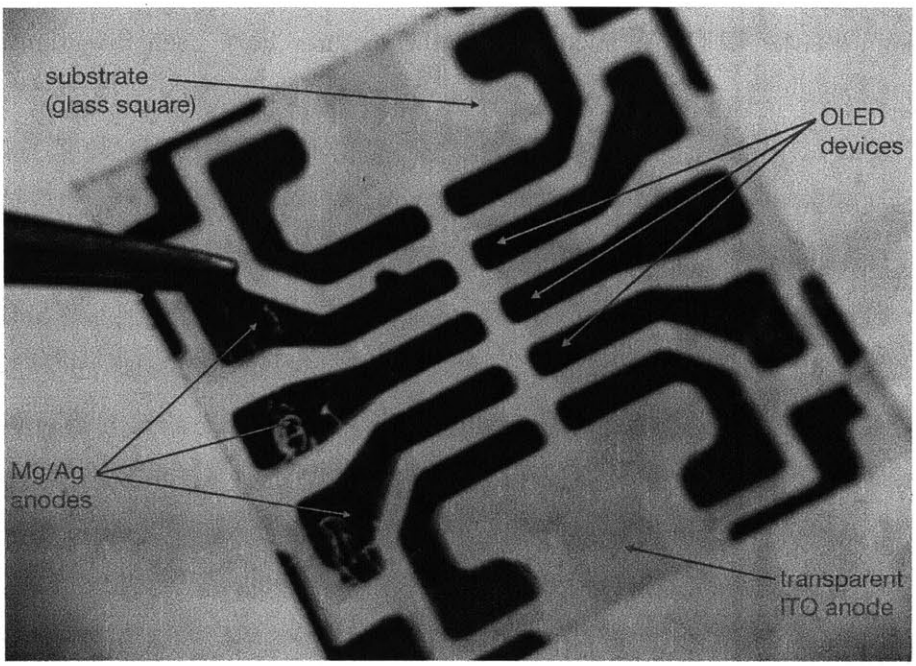

Figure 2-2: Photo of OLEDs on a square glass substrate

Note that when holes and electrons recombine to emit a photon, there is no way to tell which direction the photon will travel in after emission. The photons could travel through the sides of the OLED, or be emitted through the front, or they could go back into the cathode and be absorbed and lost. Thus, emitted light can be modeled as a set of cones coming from the active layer. A simplified diagram of this is shown in Figure 3. It is apparent that the efficiency of the LED is not very high because the direction of emitted light cannot be controlled. A light source like this is also unsuitable for applications that require a precise beam of light. Thus, structural modifications to the OLED must be made if the required light output is to be obtained.

2.2 Directionality of OLEDs

OLEDs are increasingly important for display and lighting purposes, and much research has been done about how to better control the light emitted, which would be helpful in a number of specific applications. It would also be beneficial to improve

the efficiency of the LED. As such, different structures have been investigated to determine whether the direction of emitted light can be controlled.

In [5], Feng, Okamoto and Kawata achieved highly directional emission from an OLED by using surface-plasmon tunneling. Surface plasmons are electron interactions on the surface where two materials are in contact. They can be caused to resonate by the application of light. In [5] a periodic corrugated silver film was used as a cathode, and resonance with surface plasmons on the silver aided the directional emission. This was used together with an organic material with a low bandwidth of emission, so as to have low beam divergence of the output light. They were able to alter the direction of emission by varying the grating period of the corrugated silver film.

In [24], directional emission from the OLED is achieved via an optical microcavity. The ITO anode in the OLED is replaced with highly reflective mirrors, creating an optical microcavity which is a Fabry-Perot cavity. Highly directional light was emitted from the OLED along the surfaces of a cone at around 40° from the normal. An optical microcavity was also used in [10], along with cholesteric liquid crystal (CLC) films which lined the microcavity. It was found that the CLC films improved both the emission bandwidth and directionality of the OLED. CLCs reflect circularly polarized light quite well, and this property was used to improve control of the light generated by the OLED.

Other ways to improve light output obtained from an OLED include using a metal mirror and distributed Bragg diffractor (DBR) on opposite ends of the microcavity [10]. A DBR reflects light using many layers of materials with different refractive indices. They are commonly used in waveguides [16].

2.3 OLED lifetime

One major consideration that needs to be addressed is the lifetime of OLEDs that can be made currently in the laboratory. While commercially produced OLEDs have a lifetime of hundreds of hours, laboratory-made OLEDs, made from different materials and using different packaging, last on the order of weeks. In order for laboratory-made

OLEDs to be useful in the ANN prototype, containment and packaging strategies must be devised, and investigations made into more expensive fabrication materials.

Figure 2-3a shows some lit OLEDs and Figure 2-3b shows some OLEDs near the end of their lifetime. In Figure 2-3b, the areas where the pads (i.e. individual OLEDs) are lit up can be clearly seen, however, it is also seen that parts of each device have begun to cease lighting. This occurred after the OLEDs had been exposed to air for a few hours, and they had been lit for a while. Parts of the OLED gradually stopped emitting light, and eventually the whole device ceased to emit light.

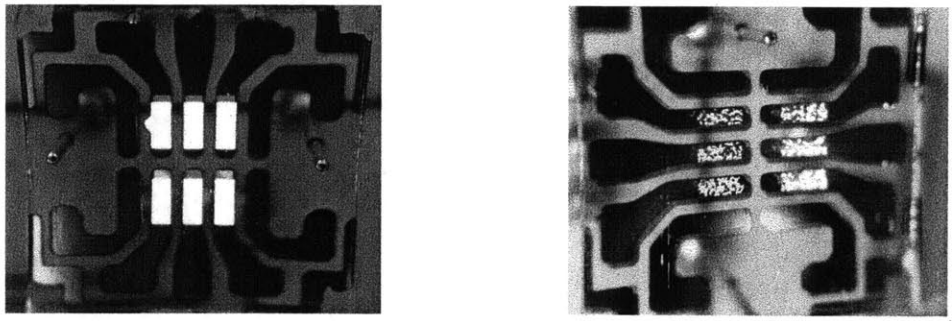

(a) Fresh OLEDs (b) Old OLEDs

Figure 2-3: Photos of lit OLEDs on a square glass substrate

2.4 State of the Art OLEDs

Much research is being conducted into OLEDs, as they promise interesting new applications, for example in televisions and in communications systems. Among the more popular reasons for this is because OLEDs can be printed onto flexible plastic substrates (instead of glass), allowing for the fabrication of flexible displays. OLED televisions are becoming popular, touted for their lower power consumption, and bright colors and the ability to make lightweight devices by using plastic substrates instead of (heavier) glass [14, 2]. As a result, there have been many achievements in obtaining OLEDs with good characteristics.

For OLEDs on plastic screens, researchers have been able to accomplish feats such as near 100% efficiency [2]. This and other research has investigated how modifying the internal structure of the OLED can allow more light to escape.

Resonant cavity OLEDs have been investigated, where wavelength-selective mirrors were placed in the OLED structure [20, 25]. This achieved greater brightness, as well as more precise control of the color of the light emitted, however, no improvement in directionality was mentioned. Other research, though, has looked into improving the directionality of emission of OLEDs (see Section 2.2).

When assessing the suitability of OLEDs for the COIN coprocessor project, I take into account current laboratory OLEDs that can be manufactured in the laboratory. The characteristics of these OLEDs are not as good as the state-of-the-art OLEDs being manufactured, but these should be kept in mind, as they could possibly be obtained for future work.

Chapter 3

Methods and Results

In this chapter, I describe the laboratory methods and processes used to fabricate OLEDs, as well as the steps taken to test the properties of the OLEDs once they were made. I also describe the procedures used to test other components that could potentially be used to build the COIN coprocessor prototype. In the corresponding sections, I then present and describe the results of all physical characterization experiments done on the OLEDs and any other components for the prototype.

3.1 OLED Fabrication

Organic Light Emitting Devices (OLEDs) are made by placing layers of materials (the electrodes, and the hole/electron providing layers) onto a substrate. A glass substrate was used for this thesis, however, commercial products often use plastic. The glass was ordered already patterned with Indium Tin Oxide (ITO) as the anode. To make an OLED, a hole transporting layer and an electron transporting layer are placed on the substrate, followed by a metal cathode. In this section, I detail the processes used to fabricate OLEDs in the laboratory (the Organic and Nanostructured Electronics Lab at MIT).

Making different kinds of OLEDs

Different types of OLEDs (made from different materials; or by a slightly different manufacturing process) can have different optical and electrical properties. Green and yellow OLEDs were experimented on, as well as green and yellow OLEDs patterned with grooves by a process called 'Elastomeric Contact Patterning' described in [18] and summarized in Section 3.1.1. Green OLEDs were made by using a hole transporting layer of TPD (triphenyl diamine or N, N'-diphenyl-N, N'-bis(3-methylphenyl) 1, 1'-biphenyl-4, 4' diamine) and an electron transporting layer of Alq_3 (tris(8-hydroxyquinolinato)aluminium), while yellow OLEDs were made by using a hole transporting layer of DCM (4-(dicyanomethylene)-2-methyl-6-(p-dimethylaminostyryl)-4H-pyran) and an electron transporting layer of Alq_3.

3.1.1 Processes Used

Thermal Evaporation

The organic materials were evaporated onto the substrate using Thermal Evaporation (physical vapor deposition, PVD) [1]. A diagram of the apparatus used is shown in Figure 3-1a, and a photo in Figure 3-1b. In thermal evaporation, materials are placed in containers (called boats), which are inside a vacuumed chamber, and heated by passing a voltage through the boat. This causes the materials to evaporate. The substrate (onto which we would like to deposit the materials) is rotating above the boats (to ensure even deposition) [6, 1]. The materials then sublimate onto the substrate. The rate of evaporation is carefully monitored during deposition. It is kept steady by adjusting the voltage supplied to the boats (and thus the temperature of the boats). The tooling factor is another useful evaporator parameter. It is a figure representing the ratio of material actually deposited to a reading from the evaporator, which allows one to get an accurate reading of how much material had been deposited while the deposition is being performed.

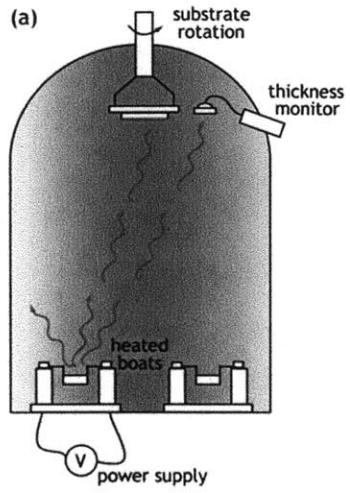

(a) Diagram of Thermal Evaporator used to evaporate materials onto substrate [1]

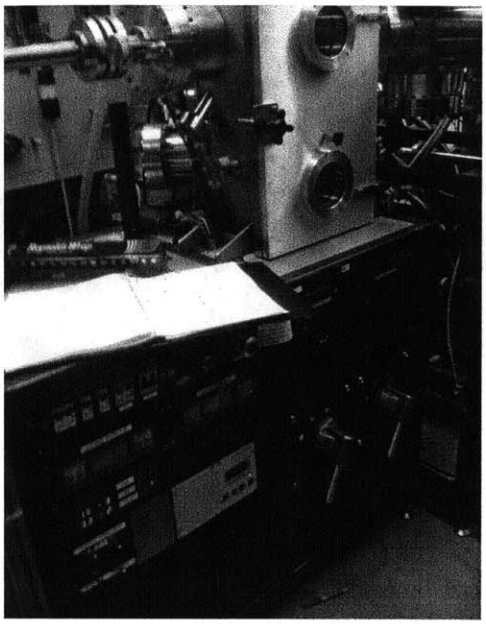

(b) Photo of Thermal Evaporator used to evaporate materials onto substrate

Figure 3-1: Thermal Evaporator in the Organic Nanoelectronics Laboratory

Spin Coating

Spin coating is a process by which the glass substrate can be evenly and thinly coated with a polymer [1, 15]. The process is illustrated in Figure 3-2 [1]. In spin coating, also called spin casting, the glass substrate is placed on a rotating stage. The solution (containing organic material) is applied to the substrate using a dropper. As soon as the solution is applied, the stage is spun (at around 500 rpm), causing the solution to be spread out by centripetal force along the substrate. The solution (which is now spread along the whole substrate) evaporates quickly after, leaving a thin layer of material on the glass. If the substrate is not cleaned well beforehand, or if the spinning is started too late after the solution has been deposited onto the substrate, there will be uneven coating of the substrate.

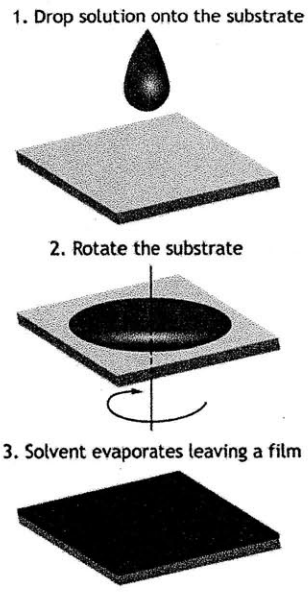

Figure 3-2: Diagram illustrating the spin coating procedure [1]

Patterning

One way to alter the light emitting properties of the OLED is to modify the internal structure of the OLED. In the experiments conducted for this thesis, OLEDs patterned with grooves were investigated to see whether patterning one of the internal layers with grooves would affect the directionality and intensity of emission.

The OLEDs can be made with grooves in the organic layers by altering the physical structure of the OLED at a micro scale level [18]. This is done by a process akin to stenciling, termed 'Elastomeric Contact Printing,' which is detailed in [18]. The result is an OLED with a layer similar to a hologram in that both have structures or grooves etched which direct or manipulate light in a particular way. A photograph of one of the OLEDs made in this way is shown in Figure 3-3. Essentially, a stamp is brought into contact with the organic layers of the device, thereby removing some of the organics as these molecules diffuse into the stamp.

The stamp is made from patterned polydimethylsiloxane (PDMS). The amount of organic material removed from the OLED is dependent on how long the stamp is in contact with the material, as well as the age of the stamp. High accuracy in

patterning can be achieved by this method, as it allows us to define features of a microscopic scale on a given organic surface [18].

Figure 3-3 shows an OLED made by this process held at two different angles to the light. The OLED is not powered, but when held to the light, its layers can be inspected. As the glass square is turned, different colors are seen on its surface. This does not happen with OLEDs that are not patterned by contact printing - no vivid colors are seen if the OLED is held to the light. The modified structure of the layer materials of the OLED reflects the light in a selective manner because the grooves reflect certain wavelengths to certain angles. It was investigated whether those grooves also directed light coming from the OLED internally (it was found that this was not the case) and also whether the grooves affected the brightness of emission (the patterned OLEDs were found to be brighter).

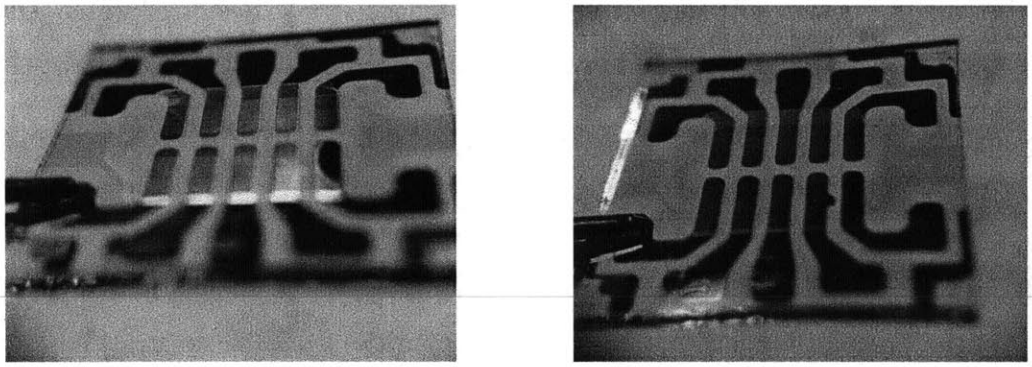

Figure 3-3: Photos of patterned OLED showing vivid colors reflected by the structure

3.1.2 Fabrication Overview

This section provides an overview of the fabrication steps detailed in Section 3.1.3. To make OLEDs, a glass substrate patterned with the anode (Indium Tin Oxide, ITO), is obtained and cleaned carefully. The electron transporting layer and hole transporting layer materials (TPD and the Alq_3 for green OLEDs) were loaded into boats in the evaporator apparatus. Some basic parameters were set on the evaporator. The glass substrate was placed in the evaporator using an evacuated system of pipelines called a transfer line.

Finally, the cathode was evaporated onto the substrate. This was done by placing the magnesium/silver material into one of the boats in the evaporator and heating them as before. In order to pattern the electrodes onto the OLED, a mask was placed over the substrate, so that the Mg/Ag electrode would only cover certain parts of the glass square (the substrate).

3.1.3 Fabrication Procedure

Detailed steps on preparing the glass substrate follow [15, 1]. A few glass substrates are prepared at a time, as it is a time-intensive process to fabricate an OLED in the lab.

1. Seven 100ml beakers were rinsed (in the appropriate solution) and filled to about 90ml - one beaker with micro90 solution, two beakers with deionized water (DI), two beakers with acetone and two with isopropanol.

2. The glass substrates were placed in a substrate holder, and lowered into a beaker of micro90 solution. It was ensured that the substrates were fully immersed.

3. The beaker (containing the substrates) was placed in a sonicator (inside the fume hood) for 5 minutes. This removes impurities from the substrates.

4. While the substrates were on the sonicator, the two beakers of propanol were placed on a hot plate inside the fume hood, and heated at 400F (to get the propanol to boil).

5. The substrates were transferred to a beaker of DI water and sonicated for another 5 minutes.

6. The substrates were transferred to another beaker of DI water and sonicated for another 5 minutes.

7. The substrates were transferred to a beaker of acetone and sonicated for another 2 minutes.

8. The substrates were transferred to another beaker of acetone and sonicated for another 2 minutes.

9. The substrates were then transferred to a beaker of (now boiling) isopropanol on the hot plate. They were boiled for 2 minutes.

10. The substrates were next transferred to the other beaker of boiling propanol on the hot plate, and again left for 2 minutes.

11. Each substrate was removed from the holder with a pair of tweezers and blasted with a puff of nitrogen, in order to evaporate any moisture left.

12. The substrates were placed, ITO side up, in a UV microwave, and exposed to radiation for 1 minute. This removes further traces of organic materials from the glass substrate.

13. Each substrate was spin coated with PEDOT (Poly(3,4-ethylenedioxythiophene) poly(styrenesulfonate)) as follows.

    - The substrate was inspected in the light to determine which side was the ITO patterned side.
    - The substrate was placed, ITO side up, on the stage in the spin caster.
    - The settings on the spin caster were adjusted to rotate at 3000 rpm for 1 minute.
    - A pipette was filled with about 60ml of PEDOT, and positioned directly over the substrate.
    - The PEDOT was deposited onto the glass with one steady press on the pipette, and at the same time, the rotation was started.
    - The coated substrate was placed, coated side down in a fluoroware container.

14. The PEDOT was removed from all areas of the substrate except the pads (the places also covered with ITO) by swabbing with a Q-tip coated with acetone.

15. The substrates were transferred to a pressurized, sterile fume hood. The substrates were placed, coated side down, into a holder.

16. The substrates were placed in the evaporator via the transfer line.

17. A hole transporting layer of TPD and an electron transporting layer of Alq_3 (for green OLEDs) were loaded into the boats of the evaporator.

18. The TPD and Alq_3 were evaporated onto the substrate with an appropriate tooling factor (obtained from the laboratory log book, based on recent evaporations). The rate of deposition was controlled to obtain a thickness of 0.5 Angstroms at 0.001 Angstrom/sec.

19. The materials in the boats of the evaporator were switched to Mg/Ag (magnesium/silver).

20. The substrates were brought back into the fume hood (using the transfer line) and a mask placed over them to provide the correct pattern for the electrodes. The substrates were then transferred back to the evaporator.

21. Mg/Ag cathodes were deposited onto the substrates using the thermal evaporator.

22. The substrates were removed from the apparatus and tested.

3.2 Characterizing and Testing OLEDs

Various characterization experiments were performed on the OLEDs. The aim of these characterizations was to obtain as much useful information about the OLED as possible, which would later be used to calculate properties of the completed prototype neural network implementation.

In this section, the optical and electrical characteristics measured or observed from the OLEDs made will be described, along with the procedures used to measure them. I will present data on their emission spectra, divergence, and how much their

intensity varies with applied voltage. It should be noted that slight variations when fabricating the OLEDs greatly affects their measurable characteristics (since a lot of the fabrication process is manually controlled). WIth practice, OLEDs can be made in a consistent manner in the laboratory. The results presented here were obtained from OLEDs made with guidance from experienced students, and so have less variation in characteristics, however, these characteristics can be easily modified.

3.2.1 Emission Spectra

Procedure

The emission spectrum of the OLED was measured in the Bulovic lab with a fibre spectrometer. The OLED was placed in a special holder, and an optical probe clamped over it. The probe was carefully aligned to be right over one (lit) pad of the OLED. Once aligned, the scan button was pressed, and the spectrometer output a stream of wavelength and intensity values.

Results

Numerical wavelength/intensity readings were obtained from the spectrometer, and a plot of the emission spectrum made. The emission spectrum of a green OLED is shown in Figure 3-4, and the spectrum for a red OLED is shown in Figure 3-5. We can see that the green OLED emits wavelengths in the range of 450 to 700 nm, with a peak intensity at around 530 nm. The red OLED emits in the range of 520 to 750 nm, with peak intensity at around 600 nm. This is consistent (in width and location) with results from other OLEDs [25]. The red OLED actually appeared yellow to the eye, and comparing the peak intensity (600 nm) with the wavelength more typical of red (650 nm) we see that the light obtained was slightly lower on the spectrum.

Small electroluminescent (EL) peaks can be seen in both plots, at 550 nm for the red OLED and 400 for the green OLED. EL peaks are caused by carriers recombining without emitting light. The wider, larger peaks observed are the photoluminescence (PL) peaks.

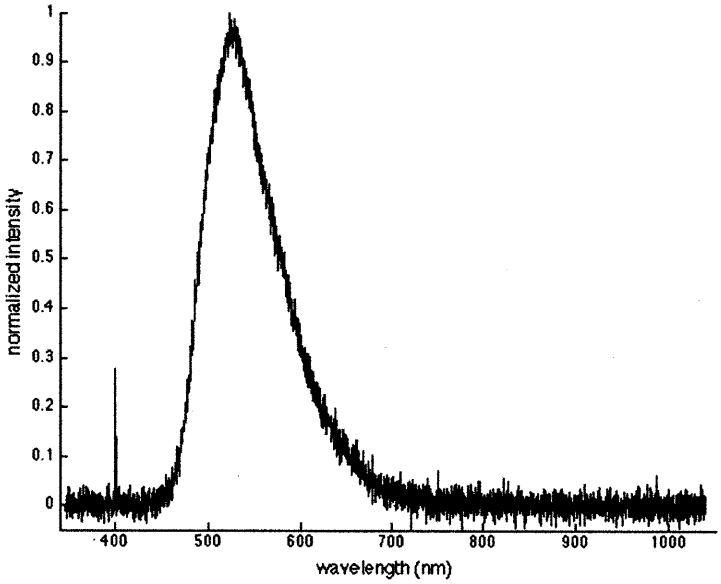

Figure 3-4: Emission spectrum for green OLED

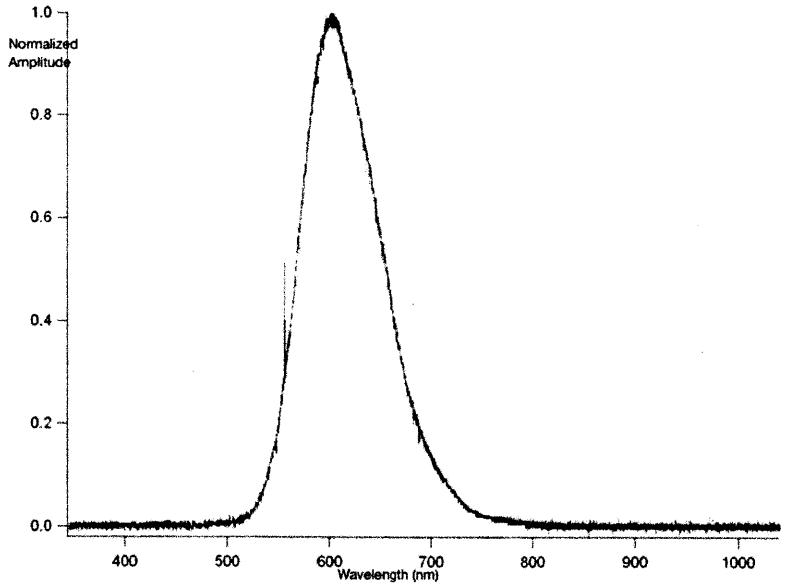

Figure 3-5: Emission spectrum for red OLED

3.2.2 Lens Evaluation of Emission Spectra

Procedure

A more visual experiment was performed with the OLEDs. Light from the OLEDs was focussed with one lens, then passed through another lens in order to collimate it. This light was then passed through a diffraction grating, and the result observed on a plain background to see if any spectral smearing occurred (i.e. if different colors were visible).

Results

When the light was passed through focussing and collimating lenses, and then a diffraction grating, very faint light was observed on the viewing screen. The output from the grating showed several images, with a spacing of about 2cm (the light was faint and so this was difficult to measure) that was in accordance with the calculated spacing for that wavelength and grating. The light emitted from the OLED was green to the eye, and the diffracted light was also green. Other colors were not distinguished from the screen (i.e. no spectral spreading was observed).

The calculations for the spacing of the images from the grating are as follows. d is the spacing of slits in the grating, λ is the wavelength of light used, θ_m is the angle between the m^{th} maxima detected and the normal to the grating.

$$
\begin{aligned}
d\sin\theta_m &= m\lambda \\
\theta_m &= \arcsin(\frac{m\lambda}{d}) \\
&= \arcsin(\frac{m \times 528\ nm}{2 \times 10^6\ m}) \\
&= 15.3^\circ \\
spacing &= 6.8 \times \arctan(15.3^\circ) = 1.9\ cm
\end{aligned}
$$

3.2.3 Divergence

Procedure

The divergence of the OLEDs needed special attention to measure. After a preliminary rough assessment (by viewing the OLEDs with the eye at different angles), a more formal experiment was set up to quantify the divergence. Measurements were taken of intensity of light emitted as the viewing angle of the OLED changed using the setup shown in Figure 3-6. Essentially, the light detector was placed in a fixed position, and the OLED was placed a known distance away from it. The angle between the OLED surface and the light detector sensor was varied, and the resulting intensities monitored. The purpose of this experiment was to measure the width of the cone of light emitted from the OLED.

The specific setup and procedure was as follows:

1. The OLED test PCB was clamped to a vertical optic mount, as shown in Figure 3-6b.

2. The mount was then attached to a rotating platform (Figure 3-6b), whose rotation was controlled by a small knob in one of its corners. The platform was marked in degrees so that the angle turned could be monitored.

3. The light detector was placed so that its light sensor was parallel to the PCB surface. It was ensured that the rotation worked fully, so that the PCB could be turned through 180°, where the PCB could be perpendicular to the sensor, parallel to it, and perpendicular to it again (but facing the opposite direction).

4. Both the rotating platform and the light sensor were bolted to the table to prevent movement during the experiment.

5. The OLED was attached to its designated place on the PCB. Care was taken to place the OLED in the center of the PCB, directly above the center of rotation of the rotating platform. This was to ensure that the distance between the OLED and the sensor did not change as the PCB was rotated.

6. The distance between the center of rotation and the light sensor was noted.

7. The PCB was connected to a power source.

The experiment was then performed as follows:

1. The power source was turned on, and the OLED inspected to ensure its pads were lit.

2. The room overhead lights were shut off, and the indicator LED of the power source was covered in aluminum foil (so that it would not affect the intensity readings).

3. The OLED was temporarily turned off and the ambient light intensity reading of the room was noted. This will later be used as a base reading to correct the raw results.

4. The OLED (mounted on the PCB) was rotated from an angle of 100° (through 0°) to $-100°$ in increments of 2°, noting the intensity reading on the light meter every time.

5. The OLEDs were covered with aluminum foil such that light only left one OLED, through a pinhole in the foil, and the previous step repeated. The foil was then removed.

6. The voltage supplied to the OLED was varied (by 1-2 V) and intensity measurements retaken for a few angles.

Two types of OLEDs were tested in this manner. The first OLED was an OLED fabricated as described in Section 3.1, except with a ITO/NPD/Alq3:DCM/Alq3/Ag:Mg/Ag stack, so that the color of emission was yellow (the materials used are for a red emission, however, the balance of these materials that actually get evaporated onto the substrate affects whether the OLED appears red or yellow when lit). The second type of OLED analyzed was an OLED patterned with 606 nm grooves. Besides gaining information about the divergence, this experiment also sought to find out whether the grooves would improve directionality of the OLED emission.

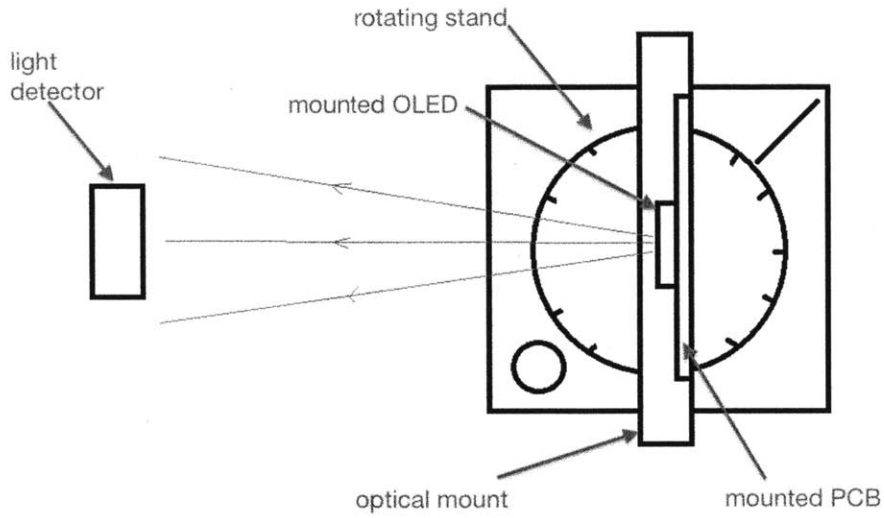

(a) Diagram of experimental setup

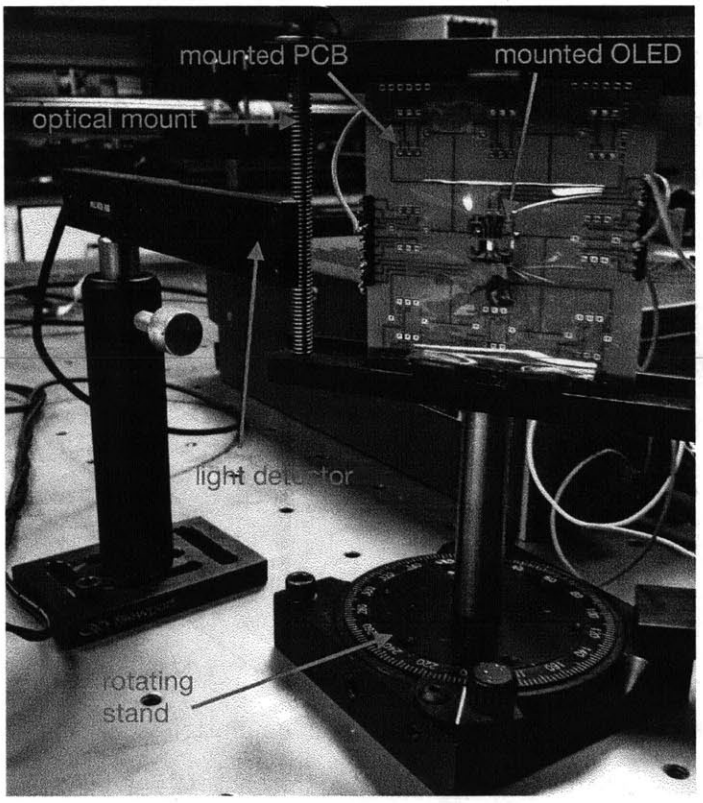

(b) Photo of experimental setup

Figure 3-6: Experimental setup for measuring OLED divergence

Results

Preliminary scans for divergence (viewing the OLED with the eye at different angles) showed that the OLEDs had a large divergence, as light could be seen from the front and sides of the devices. The empirical results are presented in Figure 3-7.

In Figure 3-7, both plots are adjusted to take into account the ambient light intensity of the room. The adjustment consisted of subtracting a base intensity reading from the raw results. Additionally, it should be noted that the regular OLED had 6 pads lit, while the patterned OLED had 5 lit (to see both plots adjusted as if each had 3 OLEDs lit, refer to Figure 3-18. Measurements were also made with a single OLED device powered - see Figure 3-8.

From this graph, one can see that the OLEDs are quite divergent (a nonzero light amplitude is detected at angles as wide as 90° (i.e. viewing the OLED perpendicular to its main direction of emission). The intensity of the light emitted clearly increases as the detector moves from being perpendicular to the OLED to being full-on in front of it. There is maximal light incident on the detector when the OLED is right in front of it. An interesting observation from Figure 3-7 is that the peak brightness of the patterned OLED is much higher than the regular OLED (the patterned OLED is 38% brighter). This is explored further in Section 3.2.6.

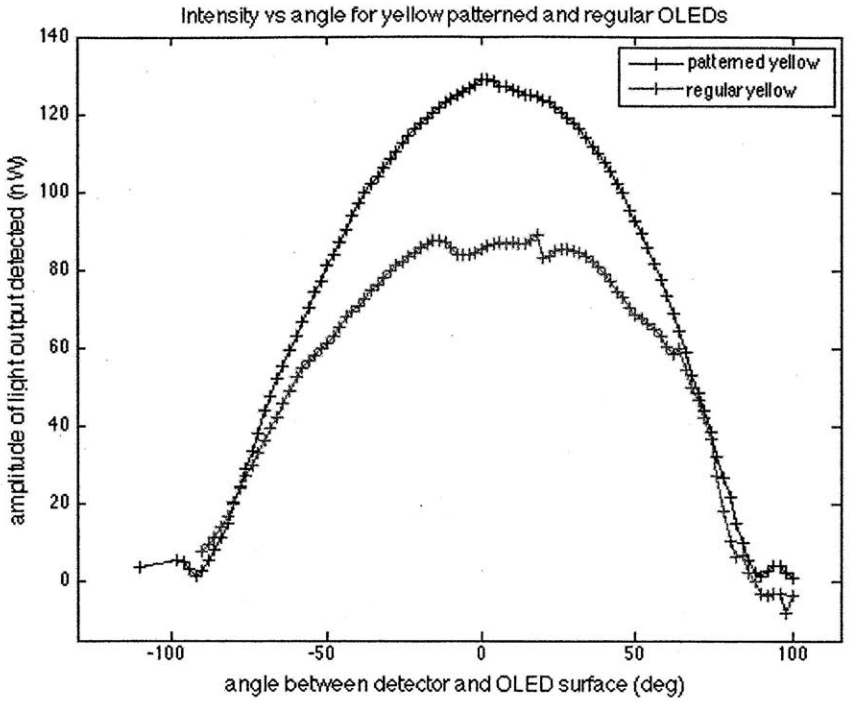

Figure 3-7: Divergence measurements for regular and patterned OLEDs

The voltage was cut off to all the pads except one, so that the intensity measurements for a single lit OLED device could be taken. The results are shown in Figure 3-8 for a green patterned OLED (the plots for two separate OLED devices is shown), and Figure 3-9 for a yellow non-patterned OLED.

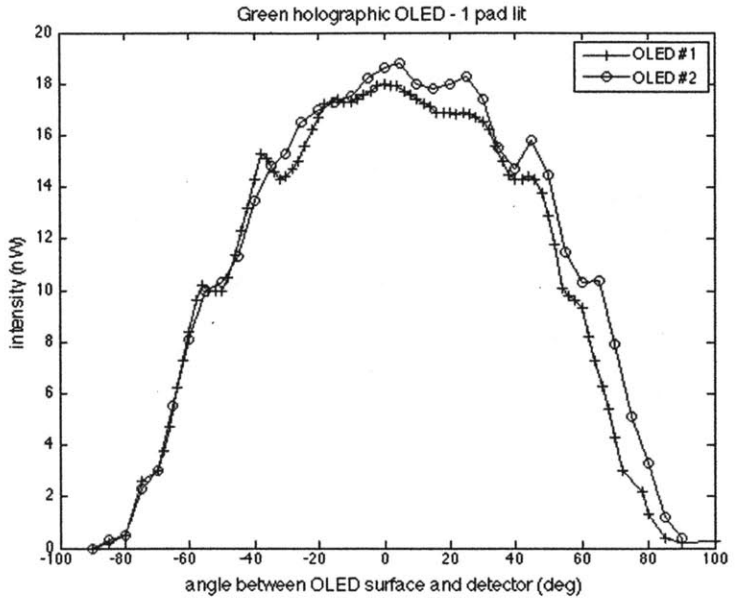

Figure 3-8: Divergence measurements for single green patterned OLEDs

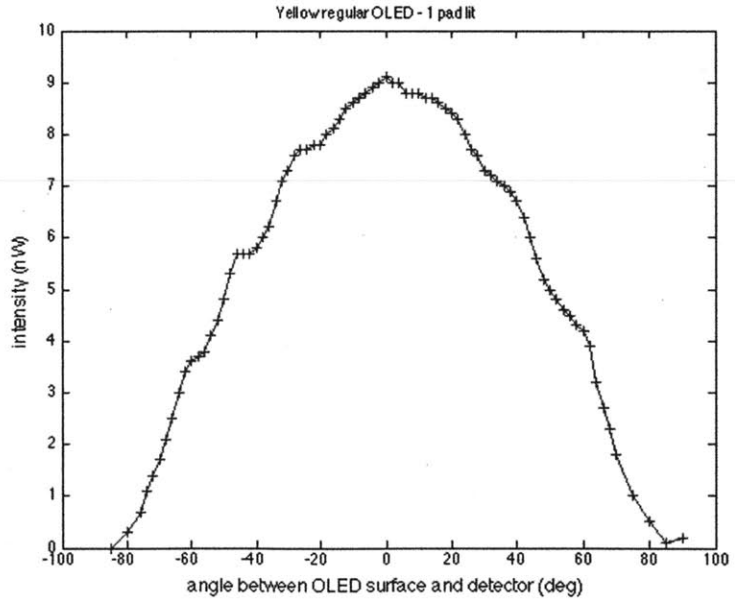

Figure 3-9: Divergence measurements for single yellow patterned OLED

The angle/intensity measurements were repeated using a pinhole to allow light to leave the (patterned) OLED. A pinhole (diameter 0.47 mm, compared to the device's

0.95 mm width) was placed over a lit OLED, and the divergence measurements taken. The results are shown in Figures 3-10 and 3-11.

The curves basically follow the intensity pattern obtained with no pinhole, but are a lot more jagged. Since the pinhole diameter is smaller than the OLED width, and the fact that the light must travel through the glass substrate before entering the pinhole, this jaggedness shows the diffraction of light through the pinhole. The jaggedness could possibly have also been because of the foil not adhering uniformly to the OLED surface. The amplitude of the light is also greatly reduced by blocking out the light from the other OLEDs on the substrate and only allowing the pinhole light through.

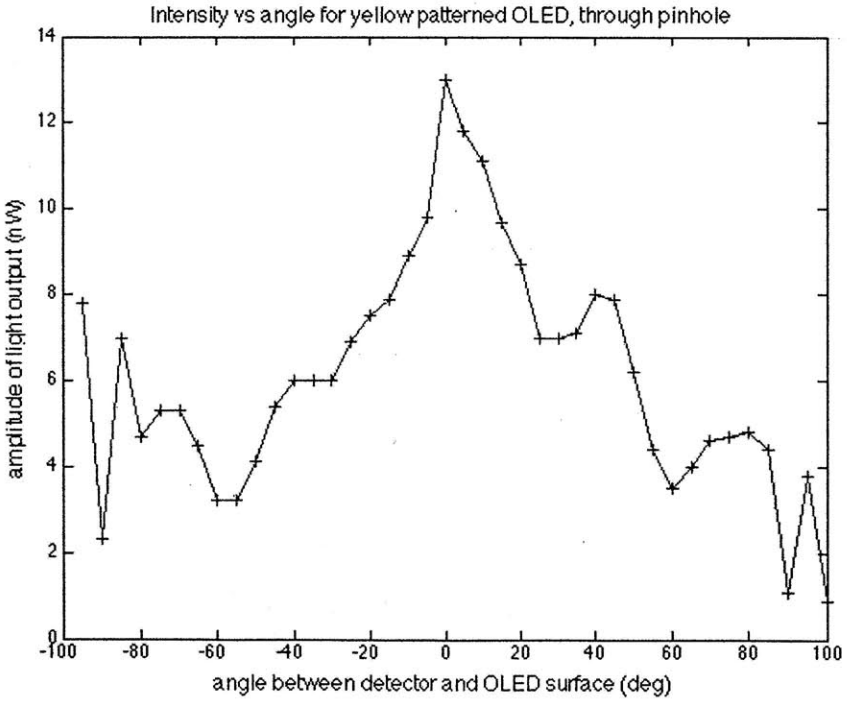

Figure 3-10: Light output vs viewing angle for yellow patterned OLED through pinhole

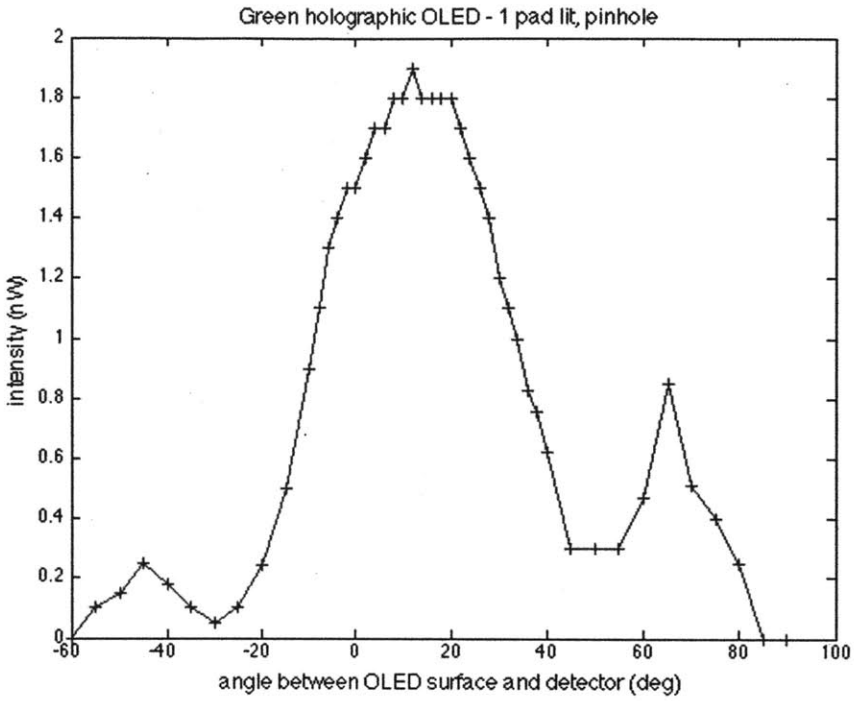

Figure 3-11: Divergence measurements for single green patterned OLED with pinhole

3.2.4 Effect of input power on output intensity

Procedure

The apparatus was set up as for the divergence experiment, with the OLED mounted at a fixed distance from the light detector. The angle was set to 0° so that the OLED was directly facing the light detector. The voltage was then varied and the output light intensity noted. The voltage was lowered until the OLED turned off, and raised until the OLED was operating at normal brightness (care was taken not to raise the voltage until the OLED burned out).

Results

Figures 3-12 and 3-13 show the effect of varying the power input to the OLEDs on the brightness of light they emit. The power input was varied by varying the voltage supplied to the OLED. The upper limit to the voltage supplied was not explored

in order not to burn out and destroy the OLED. The intensity increases roughly exponentially with voltage.

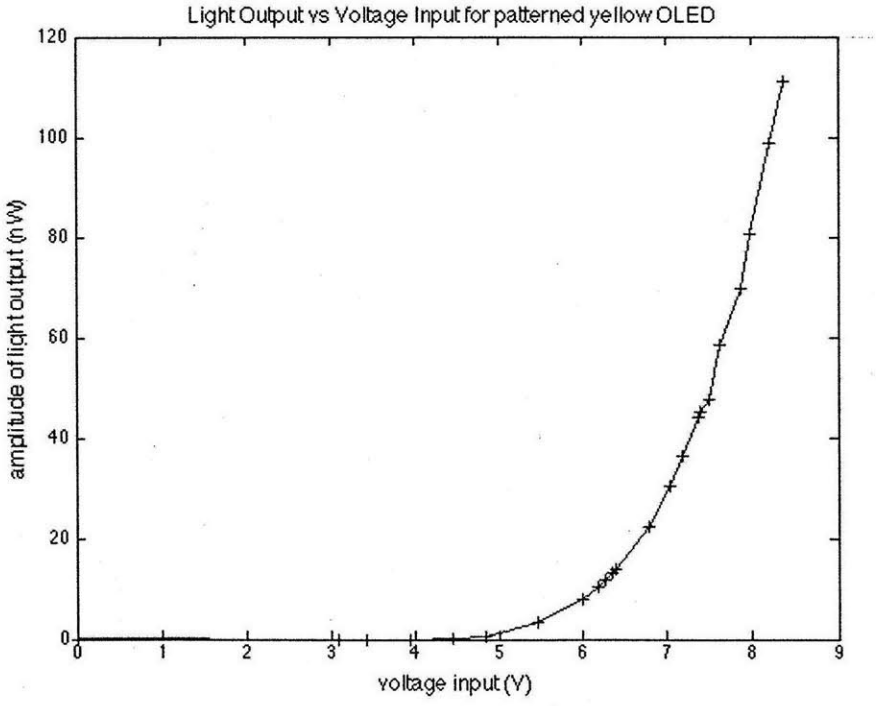

Figure 3-12: Light output vs Voltage input for yellow OLED

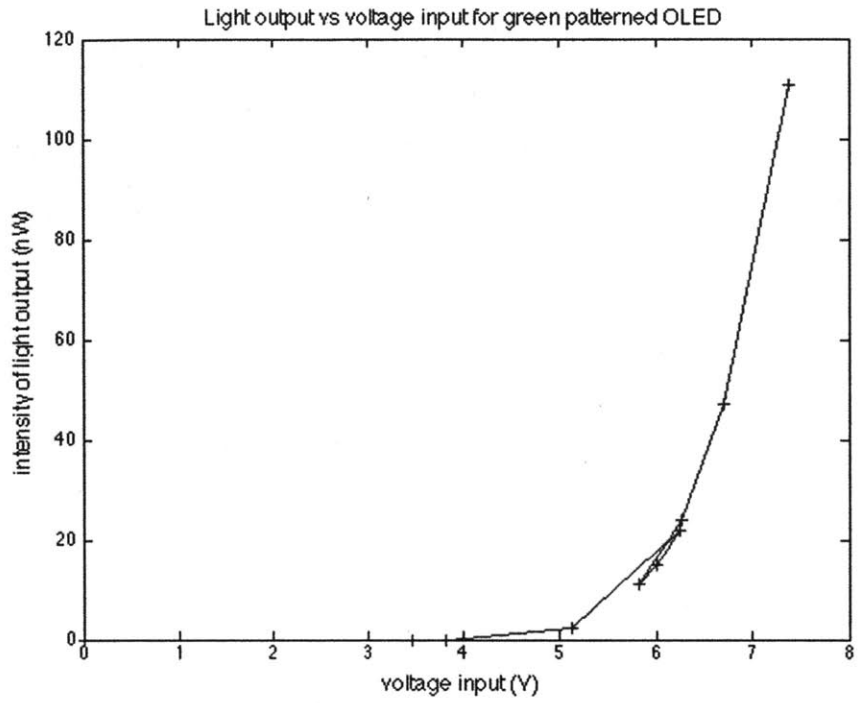

Figure 3-13: Light output vs Voltage input for green patterned OLED

3.2.5 Electrical Testing of OLEDs

Procedure

The main electrical characteristics measured were the voltage-current (IV) characteristic of the OLED, the power consumed per unit area of the OLED, and the turn-on voltage of the OLED.

To measure the IV characteristic, the OLED was placed in a test fixture which was connected to a power supply and a meter. The meter automatically varied the voltage across the OLED and monitored the current through it. The meter also gave a reading on the power consumed by the OLEDs per square centimeter (this will be useful in future calculations).

Results

The IV characteristics of the OLEDs were investigated with a meter in the laboratory. The meter measured the current drawn by these OLEDs per square centimeter at different voltages. Two OLEDs on the glass substrate (referred to as 'pad 6' and 'pad 7' on the graph) were analyzed with the meter. For a green OLED, the IV graphs obtained are shown in Figure 3-14. Here we can see that operating the OLEDs at 10V, for example, can draw different currents from different OLEDs - pad 6 required 0.037 A/cm^2 while pad 7 required 0.065 A/cm^2. Care must be taken to use appropriate margins when calculating power consumed by an array of OLEDs.

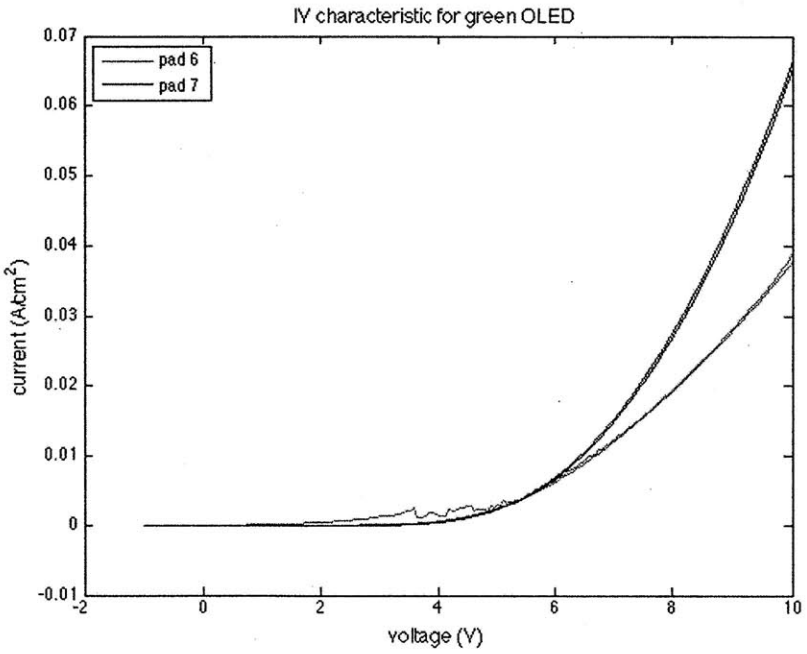

Figure 3-14: Meter output - IV curve for green OLED

The OLED was turned 15° from the detector, and the brightness measured as the voltage was gradually reduced until the OLED turned off. From this, it was determined that the turn on voltage for a non-patterned OLED (from this batch) was 5.42 V. Another general observation can be made that even though the non-patterned OLED is also turned from the detector, it is significantly dimmer than the patterned OLED at these voltages.

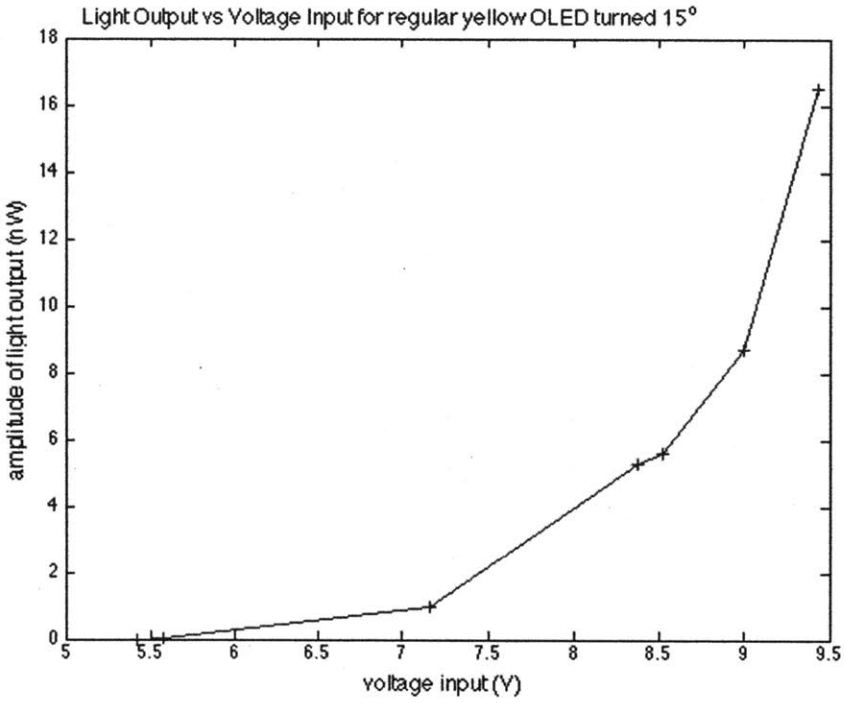

Figure 3-15: Light output vs voltage for yellow non-patterned OLED turned 15°

3.2.6 Characteristics of Alternative OLEDs

Several types of OLEDs were fabricated during the course of the experiments. Variations included different colors of OLED (green and red/yellow) and different types (OLEDs patterned with grooves and OLEDs grown without any additional structure). The emission spectra of the different colors seem consistent, and no great changes were observed. The divergence also appeared to be standard, with all variations of OLEDs still emitting light at wide viewing angles. It was found, however, that the patterned OLEDs were able to emit much brighter light than the regular OLEDs, and also operated at a much lower voltage. This will be important in making more efficient OLEDs for the prototype neural network.

Figure 3-16 shows a comparison of green regular OLEDs with green patterned OLEDs. Each of these was tested with the same voltage applied to the plate (7.4 V) and with the same number of pads (OLED devices) lit on each plate (3 lit). It can be

clearly seen that the patterned OLEDs were much brighter than the OLEDs without patterning - by a factor of at least 3.5. The voltage applied to the patterned OLEDs was decreased until they emitted with the same brightness as the regular OLEDs. This occurred at 6.24 V, which suggests that the patterned OLEDs can emit with the same brightness while using 1.14 V less.

Figure 3-16 also serves to illustrate the variability in characteristics than can be obtained with minute differences in the OLED fabrication process. Multiple OLEDs were measured and the results appear consistent in terms of the tendency of the patterned OLEDs to be significantly brighter than the regular OLEDs at the same voltage. However, we can also see that the peak brightness obtained by patterning varies by as much as 20 nW.

Additionally, as can be seen in Figure 3-16 , the patterning did not appear to affect divergence - in both the regular and patterned OLEDs, some light was observed even when the OLED was turned perpendicular to the detector.

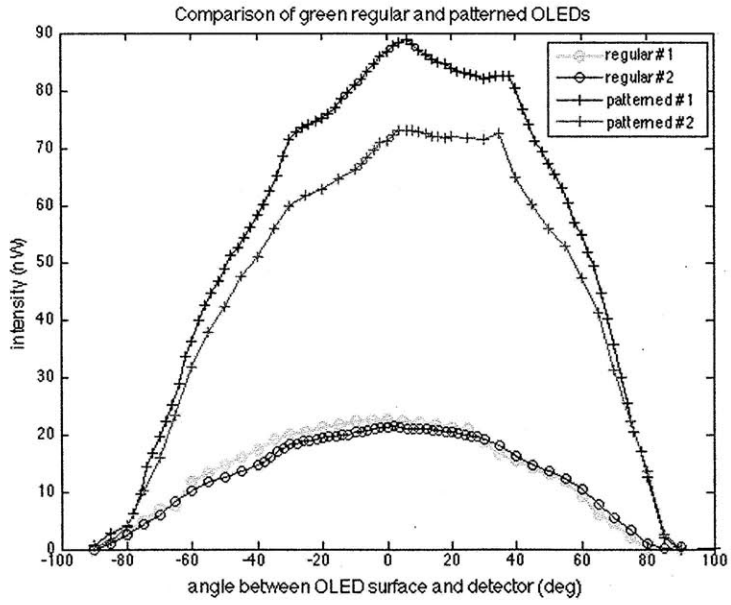

Figure 3-16: Comparison of green regular OLEDs with green patterned OLEDs

More variability was experienced when working with the yellow OLEDs. As such, it was best to compare the regular vs patterned OLEDs within the batches with

which they were made, as opposed to comparing all the batches. Figures 3-17 and 3-18 show comparisons for two batches of OLEDs made. In both sets of data, the patterned OLEDs were brighter than the regular OLEDs (though all sets were equally divergent). In Figure 3-17, we see that the patterned OLEDs are about 10 nW brighter. In Figure 3-18, we can see that the patterned OLEDs are more than 30 nW brighter, almost double the brightness of the regular OLEDs. In Figure 3-18 we can also see a lot of variability in the regular OLED characteristics. One OLED seems much dimmer than the other.

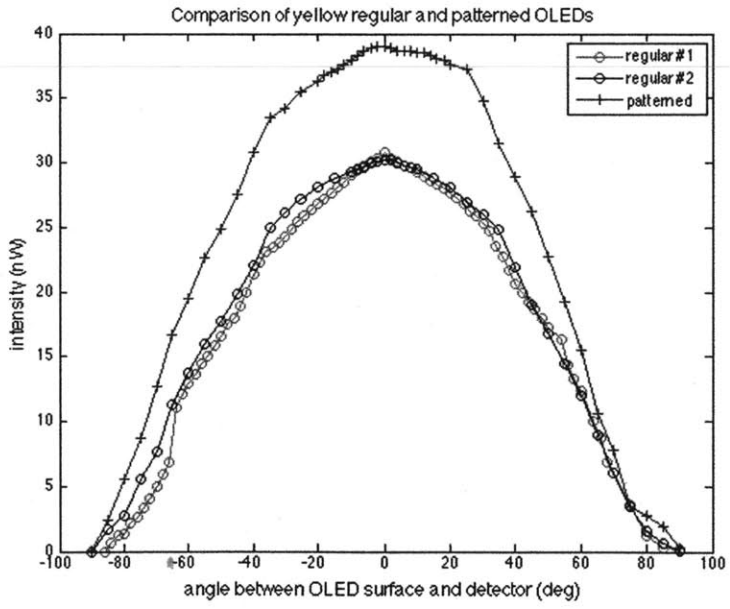

Figure 3-17: Comparison of yellow regular OLEDs with green patterned OLEDs - batch 1

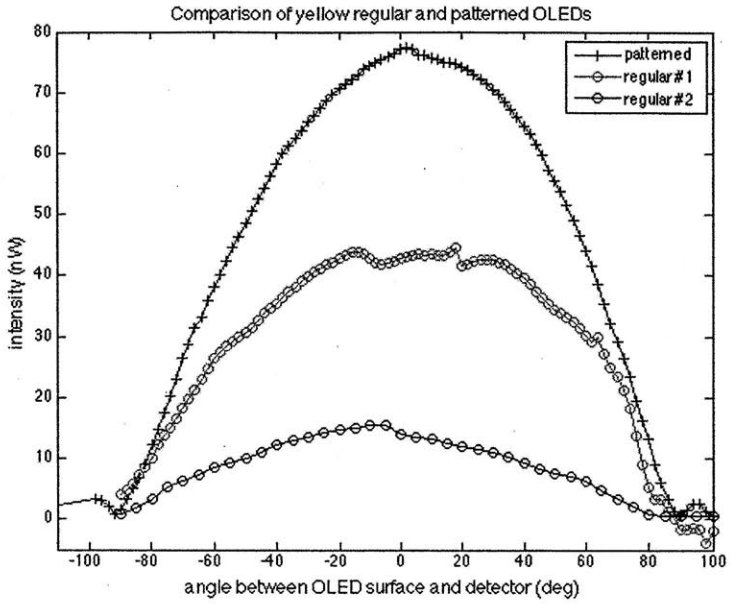

Figure 3-18: Comparison of yellow regular OLEDs with green patterned OLEDs - batch 2

3.3 Characterizing Fibre Optic Plate

3.3.1 Physical Characteristics of the Fibre Optic Plate

The fibre optic plate is meant to represent the optical interconnections between the neural network layers in the prototype. A picture of it is shown in Figure 3-19. It was made by gluing optical fibres between two plates - one plate had a 17×17 array of holes which were 1 mm in diameter. The other plate had a 17×17 array of 3×3 holes. The fibres are attached from one plate to the other in a nearest neighbor interconnection scheme - on the 17×17 side, 9 fibres leave the same hole. Each of these fibres travels to a different hole in the 17×17 array of 3×3 side. That is to say, one 'neuron' in the first layer is connected to 9 'neurons' in the second layer (as outlined in Figure 1-3).

In the 17×17 array side, the holes were 3 mm in diameter (and fit 9 fibres). In the 17×17 array of 3×3 side, the holes are each of diameter 0.5 mm (fitting one fibre each), with a spacing between holes in the 3×3 group being 0.75 mm. The 3×3

groups were separated by a spacing of 3 mm.

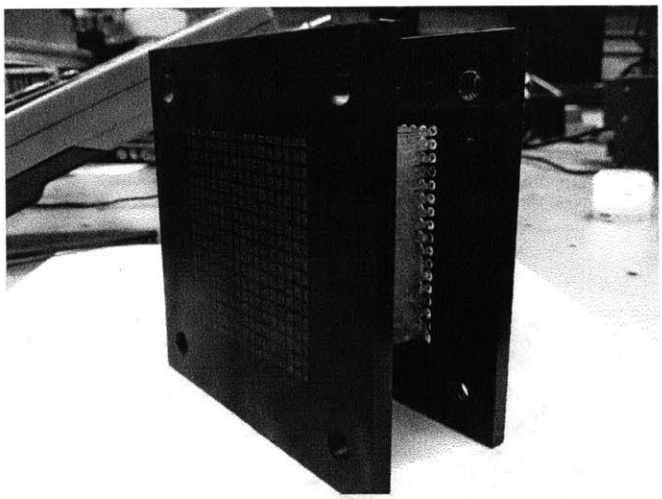

Figure 3-19: Photo of the fibre optic plate

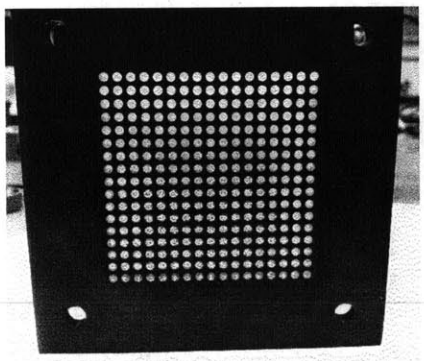

(a) Fibre optic plate - 17 × 17 side

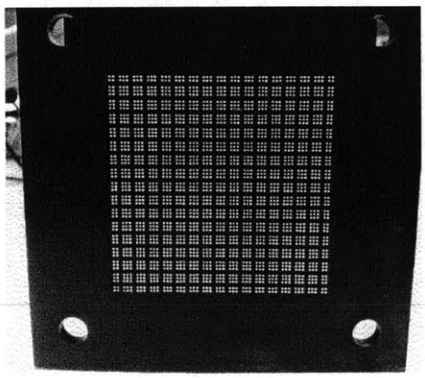

(b) Fibre optic plate - 17 × 17 with 3 × 3 side

Figure 3-20: Components of the fibre optic plate

3.3.2 Characterizing the Optical Fibre

Procedure

Various physical characteristics of the optical fibre used in the fibre optic plate were verified by measurement. The numerical aperture of the fibre is important to the calculations of power later on. This was measured with the following experimental setup, shown in Figure 3-21. A class 3B red laser was shone through a microscope objective (which diverged the light). This light was then shone into one end of the

optical fibre. The other end of the fibre was attached to a rotating stand. A light detector was placed 5.5 cm away from the end of the fibre. The angle between the fibre and the detector was then varied between 90° and -90°, and the resulting intensity recorded. From this, the numerical aperture was calculated.

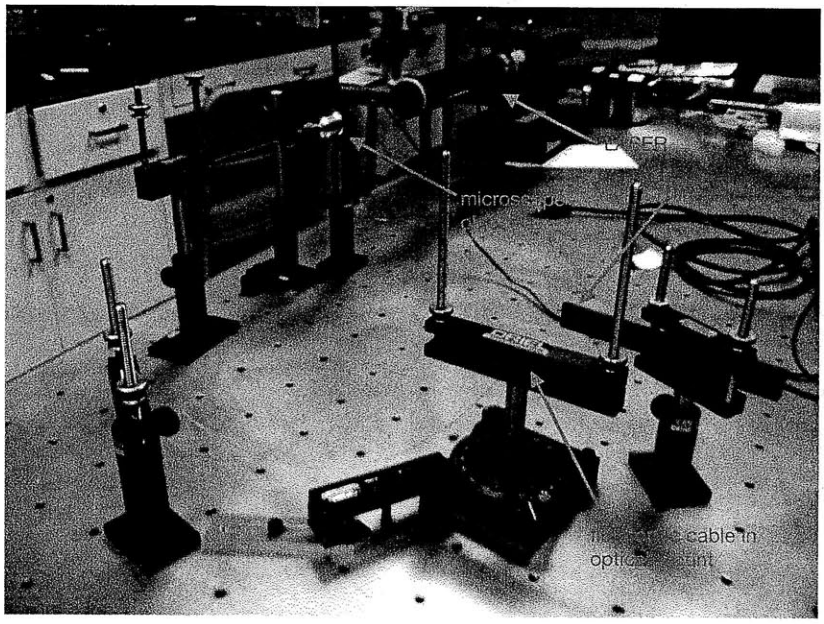

Figure 3-21: Photo of the setup used to measure numerical aperture

Results

The fibre used in the prototype was 0.5 mm thickness, cladded plastic fibre. The light measured that exited the optical fibre is shown in Figure 3-22. It is clear that the laser is much brighter, and that light emitted from the fibre has much less divergence than light leaving an OLED.

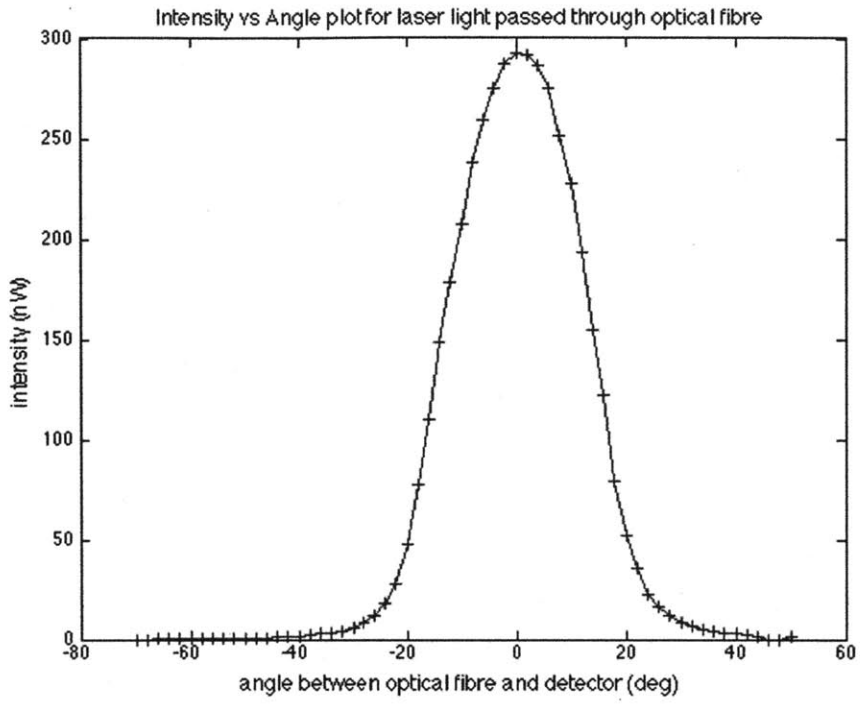

Figure 3-22: Measuring numerical aperture - Intensity vs angle for laser light through optical fibre

The numerical aperture was calculated from Figure 3-22 as follows. From the graph, it is seen that most of the light (defined as light more than 4% of peak brightness) enters the fibre between -26° and 28°. Thus, the half-angle for this cone of light is 27°.

The numerical aperture is then

$$NA = nsin\theta_{max}$$

$$NA = 1 \times sin(27°)$$

$$= 0.453$$

θ_{max} is the maximum angle at which light enters the fibre, and n is the refractive index of the medium from which the light enters, i.e. air.

Thus, the numerical aperture of the fibre was found to be 0.453. This is consistent with a number of commercially available fibres.

3.3.3 Optical Losses From Fibres

Procedure

The same experimental setup as in Section 3.2.3 was used. The angle between the OLED and the light detector was fixed. The voltage was varied and measurements of the output light intensity were noted at different voltages with and without the fibre optic plate being placed between the OLED and the detector.

Results

Figure 3-23 shows how the light intensity detected at the detector changes if the fibre optic plate is placed between the OLEDs and the detector. It can be seen that the fibre optic plate decreases the intensity by a roughly consistent amount, which was calculated to be about 5.4 nW. A photo of the fibre optic plate (from the 17 × 17 side) is shown in Figure 3-24, where 6 OLEDs were lit and placed against the other side of the plate.

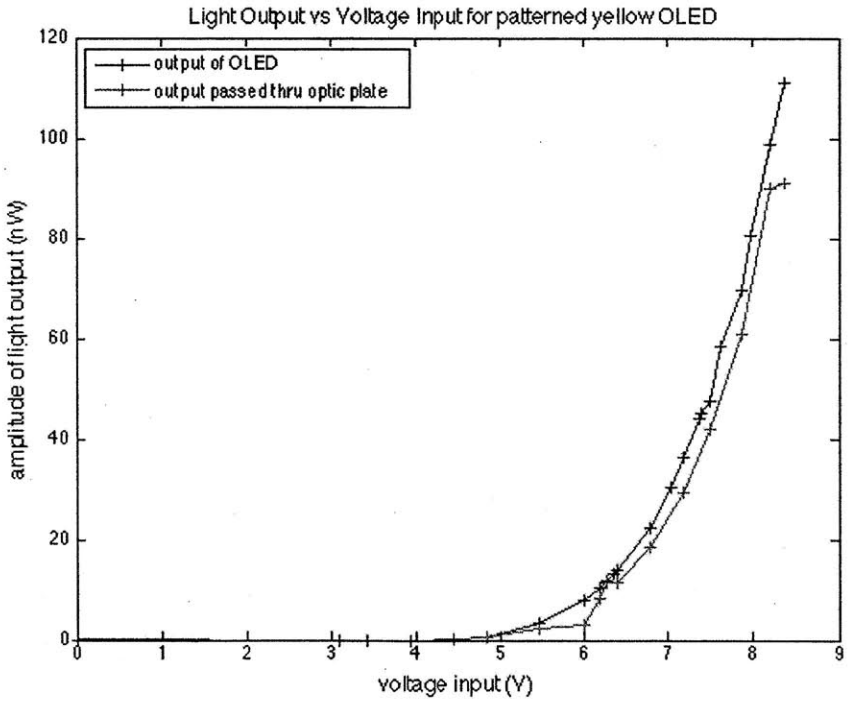

Figure 3-23: Light output vs Voltage input for yellow OLED and fibre optic plate

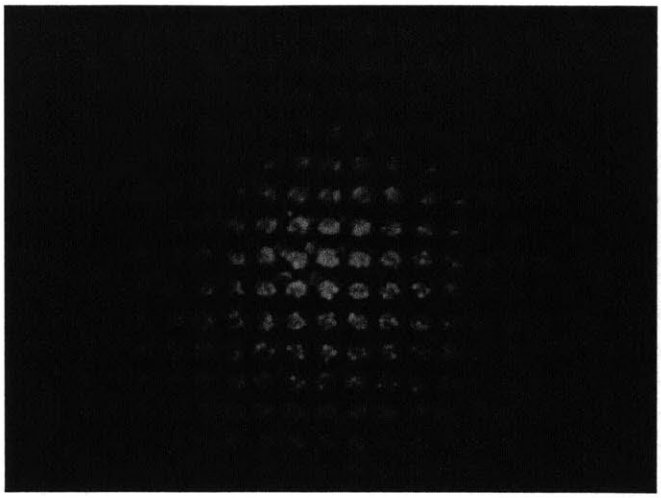

Figure 3-24: Fibre optic plate illuminated by yellow OLED

Chapter 4

Designs

The accomplishment of this project required many components to be designed. This chapter will summarize the design process, issues, and results of any parts created during this year.

4.1 Designing Testing Circuit

The main purpose of the testing circuit was to provide an easy way to power and test several OLEDs at once. It was designed to roughly emulate one 3×3 layer of a neural network (and thus hold 9 glass squares of OLEDs). In each of the squares, the overlapping of electrodes provided 10 individual OLEDs - for my designs, I assumed only the middle 6 OLED devices would be powered. So the PCB in Figure 2-2 would power $6 \times 9 = 72$ individually controllable OLEDs. The difference between what I will call an 'OLED square' versus an 'OLED' or 'OLED device', is that the square refers to the glass square substrate onto which several individual OLED devices are made (refer to Figure 2-2). All 9 OLED squares would have a common ground and power supply, but 6 OLEDs on each square could be individually controlled if desired.

The circuit shown in Figure 4-1 was designed using the PCBArtist software [4]. The ground wires are shown in yellow, while the powered wires are shown in red. The pads at the edge of the square are meant for external connectors (wires to the power source). The clusters of 8 pads in the center of the PCB are meant for the OLEDs to

be connected. Special spring pins are soldered into these holes, as a good contact is required to the OLED surface. The spring pins allow for imperfections in assembly of the board by adjusting their height easily.

One consideration involved in designing this PCB was the large number of wires/tracks required to individually control 72 OLEDs. For a 17×17 layer, this would be 289 individually controlled OLEDs, which would also require many tracks (and then many wires to the power source). To avoid lag and crosstalk, these wires should be kept short. Standard connectors and ribbon cable would also help reduce clutter.

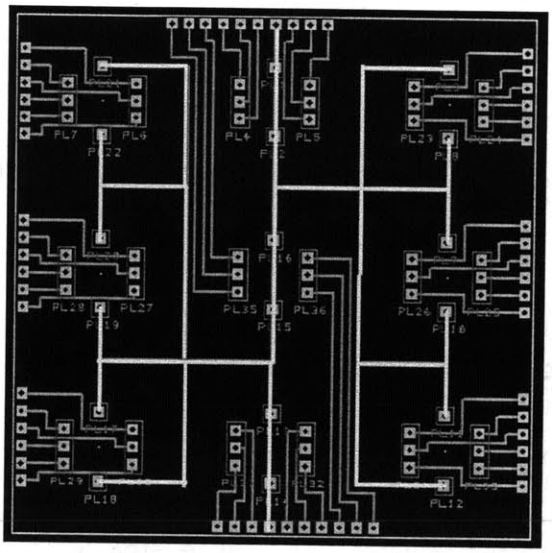

Figure 4-1: Testing circuit for OLEDs - first design

4.1.1 Evaluation of current circuit and suggestions for improvement

The current design was intended as a rough test circuit for the OLEDs available at the time (since ordering custom OLED patterns would take time). The circuit was also built with electronics readily available, rather than more ideal custom electronics. OLEDs can be made so that they are on a smaller glass plate, and the number of OLEDs per plate can be changed. If, for example, a 17×17 array of OLEDs were printed on one glass plate, the wiring for the contacts of the PCB would change drastically.

Proper alignment of the spring pins (which were individually soldered) was a concern. To get alignment, a female connector was placed on the other side of the PCB, and the spring pins were passed through the holes in the PCB and held in place by sticking them in the connector until they had been soldered into place. It would be easier (and more precise alignment would be obtained) to order or design a PCB where the pins can be attached more easily. A simple solution would be to use header pins, and stick the spring pins in those sockets.

If a seal were to be placed around the OLEDs (see Section 4.2), the PCB would have to be larger in order to have enough room to place a seal around the area of the OLEDs. The tracks would also extend to the edge of the board in this case.

4.2 Designing Packaging for OLEDs

One of the most important steps in producing a working prototype ANN using OLEDs is making the OLEDs last for a long time in air (in atmospheric or room conditions). As discussed in Section 2.3, OLEDs are very susceptible to moisture and oxygen, and will break down shortly after leaving the evacuated glovebox conditions. The OLED lifetime in air was sufficient to conduct normal laboratory tests (such as electrical and optical tests), but for an ANN prototype, the OLEDs would need to last much longer. Thus, some sort of container is needed to protect the OLEDs and increase their lifetime in air. I will outline a few of the designs discussed for making such a container.

The simplest approach to protecting the OLEDs would be to enclose them in some sort of airtight box. This box would be evacuated or flushed with nitrogen before the OLEDs were placed in it, and sealed such that a minimal amount of contaminants would enter afterwards. Since we are concerned with making a portable, lightweight prototype, the size of the box is another design constraint. Additionally, the wires to the power source need to somehow pass through the box (or, a way to provide power to the OLEDs is needed). Different designs for the box were discussed, among them, using the PCB as one edge to the box, and using an aluminum and glass casing.

One box design involves placing a glass layer above the OLEDs (to let light through) and an aluminum backing to the box. A diagram (not to scale) of this is shown in Figure 4-2. Some of the main features of this design are:

- The 'box' would actually not enclose the PCB, but would consist of a front-plate and a back-plate attached to the PCB, so as to encapsulate the OLED devices.
- The front plate would be glass (to let light pass through) resting on some sort of metal surrounding (sealed with rubber or epoxy) and the back plate aluminum, which is light, strong, and can be drilled into. Screws from the front plate to the back plate would hold the whole box together.
- The front and back plates would meet the PCB via a rubber O-ring placed on the PCB. This would ensure an airtight connection of the components.
- A pipe and valve could be included, so that the box could be connected to a pump and flushed with nitrogen. Alternatively, the box could be assembled in an already evacuated environment, eliminating the need for additional components in the box.

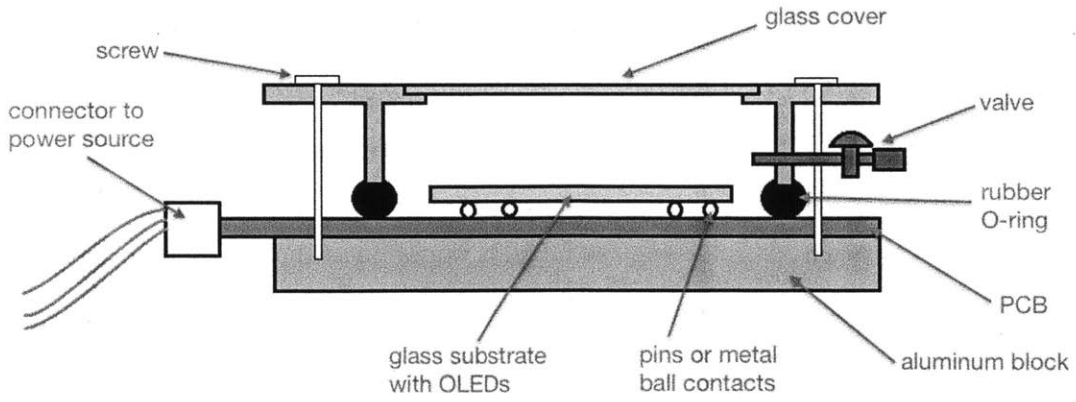

Figure 4-2: Design for container for OLEDs - aluminum backing (not to scale)

Some considerations that would have to be addressed with this design is the possibility for loss of light between the OLED and the glass plate covering the box.

The distance between the OLED and this glass would have to be minimized (and so there might not be room for the valve in the design).

Another approach involves sandwiching the OLEDs between two glass plates. Instead of the OLEDs being grown on a a few small square glass substrates, the OLEDs would be grown all on one glass plate. Then, another glass plate could be sandwiched against it and sealed with epoxy, reducing the number of plates needed to seal the apparatus. Note that special epoxy must be used, as typical epoxy is cured with UV light, and the OLEDs are sensitive to UV radiation. A new design for the ITO pattern on the glass substrate would be needed, as the tracks from the emitting area to the area used to connect to the power source would need to extend to the edge of the (larger) plate. The pattern of the tracks could resemble the pattern of the wires in the design in Figure 4-1.

Yet another approach (used in [15]) involves coating the OLED with epoxy. This seals the area around the OLED, however, it also covers the OLED, which means that any light obtained must now also pass through the epoxy layer, possibly getting distorted, or attenuated in some manner. This is likely to be unsuitable for a large number of OLEDs in the artificial neural network.

Throughout all of these designs, it must be considered whether the whole neural network prototype could be contained in a controlled environment (like a glove box) if OLEDs are to be used. Alternatively, parts of the prototype containing the OLEDs could be enclosed, or the devices could be enclosed on an individual basis, as described above.

4.3 Designing Optical Coupling Interfaces for Proposed Network

In the prototype artificial neural network, there will be consecutive layers of 'neurons', consisting of photodetectors, thresholding circuitry, and OLEDs as emitters to the next layer (which will be composed identically). This section will concern the interface

between the emitting devices (the OLEDs) and the photodetectors on the next layer.

In the current COIN co-processor prototype, efficient holographic interconnections are used between the emitting layer and the next detecting layer [22]. Light from the VCSEL laser is emitted from a 3×3 square configuration, such that there are 9 independently controlled beams of light incident on the hologram. The light is passed through a Bragg holographic array, which has gratings that direct each beam in a different direction, to the next layer, which consists of a 3×3 array of photodetectors.

It was hoped that enough directionality might be obtained from the current OLEDs such that a holographic array would no longer be needed to guide the light from layer to layer. However, obtaining good directionality from OLEDs is a nontrivial endeavor, and in lieu of these, some sort of external light guidance will be necessary. This could be in the form of a micro lens array, or holograms, or diffraction gratings.

A major consideration in choosing optical interconnections is the power loss associated with coupling the light. Thus, components must be butt coupled, but also, high efficiency components must be selected. Another consideration is the fact that the OLED light is not coherent, and is much wider in emission angle than laser light. Thus, holographic interconnections might be harder to make. Additionally, because the OLEDs have a fairly wide emission spectra, diffraction gratings may also be difficult to use. Appropriate lens arrays seem to be the easiest to use.

Chapter 5

Implications for the COIN coprocessor

In this chapter, I discuss how my findings in Chapter 3 impact the design of the prototype COIN coprocessor, in terms of the power required for such as system, and the performance expected.

5.1 Power Budget

When making calculations of the power input to and output from the OLEDs, it must be noted that there is a wide variability in some OLED characteristics, depending on the type of OLED and the experimental procedure. Thus, some margins should be taken into account when calculating the power budget.

5.1.1 Input Power Required

The input power required for one 17 × 17 layer of OLEDs was calculated as follows. The device area was measured, and multiplied by the current consumed per unit area (a constant obtained from the meter) to find the current consumed. This was then multiplied by operating voltage to find the input power. Note that the OLEDs could be operated at various voltages, so this input power could be varied. Additionally,

the proximity of the OLED to the light detector affects how much light is incident on the detector, so distance between emitter and detector should also be a consideration in these calculations.

$$\begin{aligned}
\text{device area} &= 0.0239\ cm^2 \\
\text{operating voltage, } V &= 6.5\ V; \\
\text{current consumed by OLED per area} &= 0.0087 \text{ to } 0.01\ Acm^{-2} \\
\text{current consumed by one OLED} &= area \times current\ per\ cm^2 \\
&= 0.21 \text{ to } 0.24\ mA \\
\text{Input Power Required for one OLED, } P_{in} &= V \times I \\
&= 1.4 \text{ to } 1.6\ mW
\end{aligned}$$

For a 17×17 array, the electrical power required would be 0.4 to 0.45 Watts, and for a $17 \times 17 \times 3$ array, the power required would be 1.1 to 1.3 Watts.

5.1.2 Output Power Obtained

The output optical power per OLED square (with 6 OLEDs lit) measured at a distance of 6.5 cm was about 128 nW for one of the patterned OLEDs and about 93 nW for one of the un-patterned OLEDs. Viewed through a pinhole, the brightness measured from one of the OLEDs was 13 nW at 6.5 cm. With another batch of regular OLEDs, the optical output power measured at a distance of about 0.02 cm was about 190 nW at approximately 6.5 V. There is a lot of variability in the power that can be obtained from the OLEDs, but picking one set of samples will do for an example power calculation. To get a better idea of the total optical power emitted by the OLEDs, a plate of 6 lit OLEDs was held against the light detector to achieve maximum coupling. The light intensity measured from this was 21.2 μW.

5.1.3 Efficiency

From the calculated figures, the efficiency was estimated as follows. The optical output power measured (i.e. the light intensity emitted) was divided by the electrical power required for one OLED.

$$\begin{aligned} \text{input electrical power required, } P_{in} &= 1.4 \text{ to } 1.6\, mW \\ \text{output optical power obtained, } P_{out} &= 21.2 \mu W \\ \text{efficiency, } \eta &= \frac{P_{out}}{P_{in}} \\ &= 1.4 \text{ to } 1.6\% \end{aligned}$$

These numbers are fairly low, compared to typical OLEDs. The most error prone part of the measurements taken was in the output optical power. The OLEDs are not precisely butt coupled to the detector, and because the OLEDs are very divergent, it is likely that not all the light was captured. It is thus probable that the actual efficiency is higher.

State of the art OLEDs have achieved up to near 100% efficiency, however most typically-fabricated OLEDs have efficiencies of 20-30% [2]. One area heavily researched is the use of high refractive index substrates, since a lot of light is lost traveling through the glass between the actual OLED surface and the air, because of the variation in refractive indices of the organic layers, the glass substrate and the ITO pattern [2]. As much as 80% of the light emitted by the OLED can be lost due to total internal reflection [25], thus a method to more efficiently extract light from the OLED is needed. The high efficiency OLEDs have been achieved with very high refractive index substrates, or by using very good organic polymers for the OLED layers. Obtaining of OLEDs of higher efficiency would be beneficial to building a good neural network prototype.

5.2 Electrical Requirements for OLEDs

The electrical components required for the prototype layers for which I will specify recommendations are a driver circuit to power the OLEDs (and logic to individually control them) as well as photodetectors that will detect light input to the layer. Intermediate logic to perform summing and thresholding operations in each layer is also necessary.

The driver circuit should be able to provide a maximum power of about 7 W (if all the OLEDs in all the layers were to be lit) at no more than 10 V. Depending on what type of OLED is chosen (for example, patterned vs non-patterned) this power requirement could be as much as halved.

The photodetectors used will need to be sensitive to light between 450 and 700 nm (a narrower range will be output, in reality, with ranges depending on which color of OLED is used). The photocurrent produced would be converted to voltage by a transimpedance amplifier, and this voltage would be the input for another neural layer [22]. Currently, photodetectors for this part of the spectrum are readily available from electronics distributors, so these components should be straightforward to obtain.

5.3 Requirements for Optical Interconnections

The divergent nature of the OLED emission requires some sort of light-guiding component between the OLED and the next component if a neural network prototype is to be built. In the last COIN prototype, holograms were custom made to guide the light from one layer through to the next layer. Using the divergence measurements described in Section 3.2.3, holograms could be made to direct the OLED light.

The fibre optic plate available has a wide acceptance angle (large numerical aperture) which is good for accepting the OLED light, however, if we want it to accept light selectively, a plate should be made with a smaller acceptance angle. We might want to accept light more selectively because the OLEDs are very divergent - a smaller acceptance angle means we are more certain that the light input to a particular fibre

came from the OLED we wanted it to come from.

5.4 Comparison of OLEDs with VCSELs

There are certainly tradeoffs to be made in the design decision to use OLEDs vs Vertical Cavity Surface Emitting Lasers (VCSELs). VCSELs offer several advantages in that they produced focussed and coherent light with only little divergence. The output optical power of the light emitted is also very high, and thus the beams are very bright. Lasers emit coherent light, which makes the use of holograms and other light-guiding components easier. VCSELs are also easy to place into 2D arrays [19].

A key disadvantage of VCSELs lies in their power consumption. VCSELs require a lot of power for the laser to turn on and start emitting light. For a neural network type architecture, where there are many layers of 17×17 (or more) lasers, each of which must be turned on and off frequently, the power consumption is massive. OLEDs, on the other hand, require much lower power on average, and can be turned on and off easily, consuming far less power.

Another disadvantage of VCSELs is their high cost. The materials (hybrid silicon/gallium arsenide) are expensive to procure, and custom designs are also harder to make. OLEDs, on the other hand, are much easier to procure, though they quality and characteristics of OLED desired can greatly affect this.

Table 5.1 highlights some of the physical differences in characteristics of state-of-the-art OLEDs vs OLEDs that are currently made in the laboratory vs a typical commercially available VCSEL.

	state of the art OLEDs	laboratory OLEDs	typical VCSEL (sample)
divergence	40°	180°	16° - 30°
operating wavelength (nm)	400-750 (variable)	450-750 (variable)	650-1300 (GaAs)
spectral width (nm)	200	200	<1
output power	42 mW	10 - 20 μW	10 - 20 mW
efficiency	60% (typical) ≈100% (max)	1.4-1.6%	45%

Table 5.1: Comparison of typical OLEDs, laboratory OLEDs and VCSELs [19, 17, 24]

We can see from Table 5.1 that the VCSEL has the narrowest divergence. All 3 of the devices have different operating wavelengths, depending on the properties of the materials used in their manufacture. Additionally, the lasers have a much narrower emission spectrum (and more coherent light) than the OLEDs. It can also be seen that the lab lasers are very inefficient, but that higher efficiency from OLEDs is certainly possible.

Chapter 6

Conclusion and Recommendations

From this project, several questions are raised about the potential of OLEDs in the COIN coprocessor prototype. Among some of the main questions answered were the suitability of OLEDs, in terms of power requirements and optical characteristics. In this chapter, I summarize the findings made and describe some areas that could be useful to investigate for further designs.

6.1 Overall Implications for COIN coprocessor

As a conclusion to the investigations made, OLEDs would have several benefits if used in the COIN coprocessor prototype. Less power would be required, and a more compact custom design could be built. However, much care would have to be taken in designing optical interconnects because of the divergent nature of OLED light.

6.2 Areas to look into

6.2.1 Directionality

One of the most important areas would be to continue to investigate the degree to which using directional OLEDs can reduce the amount of optical light-guiding hardware needed in the prototype. Directionality in OLEDs is a lofty goal, however,

slight modifications to the OLED structure can have beneficial results, as seen in the experiments described in this thesis, where patterned OLEDs were much more efficient than plain OLEDs. This has promising implications for making a prototype that requires much less power. If more directionality can be achieved, a much more compact prototype can be built, since less equipment would be required to guide the light.

6.2.2 OLED Structure

Different methods of manufacture, as well as methods to alter the structure of the OLEDs should be explored, and current research in the field incorporated. Several aspects of OLEDs have been investigated by researchers, such as resonant cavity OLEDs [20, 25] and OLED patterning [18]. This resonant cavity research obtained greater brightness and more control over the emission spectrum, but not directionality, or increased coherence. Other optic cavity research (also using small mirrors in the OLED structure) has managed to improve directionality [24], and this could be further explored. Patterning, as investigated in this thesis and in [18] could also be useful in increasing brightness obtained and in producing more efficient OLEDs, reducing the power consumed by the network.

6.2.3 OLED Lifetime and Packaging

Another important characteristic is OLED lifetime. This can be lengthened by using different materials in the manufacture of the OLEDs, or by designing non-cumbersome packaging to seal the OLEDs from air, as discussed in Section 4.2. Increasing the OLED lifetime would allow the ANN prototype to run for lengthy periods without having to replace the OLEDs.

Major considerations when designing packaging for the OLEDs include ensuring the light from the OLEDs is coupled out efficiently, the need to be airtight to preserve the OLEDs, and the need to be easily assembled and disassembled inside the glovebox or another controlled environment. One of the ways to package the OLEDs discussed

in this thesis would be to enclose the OLEDs in an airtight box, with a back plate of aluminum and a front plate of glass. A valve could optionally be included to evacuate the box. Another way was to enclose the OLEDs between two glass plates sealed with rubber and epoxy.

6.2.4 OLED Efficiency

High efficiency OLEDs are a greatly researched topic. Processes and materials used to make high efficiency OLEDs are often proprietary or expensive, but simple modifications such as patterning can also produce good results. While OLEDs generally do not consume much power, a neural network prototype will involve lots of devices, and it would be advantageous to get maximal output for as little power as possible.

6.2.5 Optical Interconnections

More research into the characteristics of the fibre optic plate would help in determining the system limits in terms of the minimum output power required from the OLEDs. In this way, the power consumed by the network could be reduced. A lossy fibre optic connection would be undesirable in the prototype. While using optical fibres gets rid of the crosstalk of electric wires, they are still susceptible to leakage of light between fibres. Choosing a good fibre and layout is essential.

6.3 Conclusions

Organic Light Emitting Devices are versatile, customizable, and provide a variety of favorable characteristics for use in the prototype artificial neural network. Through the experiments conducted and background research performed, it is clear that OLEDs are capable of offering much in the building of the artificial neural network prototype. Among the benefits are easy manufacture, fair degree of customizability both in terms of OLED structure and of making different sizes of arrays of OLEDs, low power consumption, and quick turn on times.

VCSELs as currently used in the ANN prototype also offer advantages - focussed, coherent light with a good intensity. The main disadvantages of VCSELS are that they require a lot of power, and there is a lag in their turn on times as they take a while to start emitting. Materials for VCSELs are also expensive. OLEDs are cheaper, require less power and can turn on and off with less delay.

Given the amount of research conducted into OLEDs it is certainly possible to achieve very good characteristics, and to have higher efficiency and more focussed light than was obtained from the experiments conducted. However, VCSELs are easy to obtain (through suppliers) while OLEDs must be carefully manufactured (and their properties depend heavily on the nuances of the experimental fabrication). More consistency between samples is obtained from ordering commercial VCSELs rather than from making OLEDs in the laboratory.

In conclusion, OLEDs have many benefits to offer the prototype neural network. However, care and time would need to be invested in finding OLEDs with the right properties that can be made easily in the laboratory. VCSELs have been proven to work in previous prototypes, and are easily obtainable. However, they have a few drawbacks, which could ideally be improved upon with carefully designed OLEDs. If an immediate prototype is needed, available VCSELs should be used. Moving forward, however, the continued research into obtaining OLEDs with better properties would lead to great benefits.

Bibliography

[1] Polina Olegovna Anikeeva. *Physical Properties and Design of Light-Emitting Devices Based on Organic Materials and Nanoparticles.* PhD dissertation, Massachusetts Institute of Technology, Department of Materials Science and Engineering, 2009.

[2] Wang Z. B., Helander M. G., Qiu J., Puzzo D. P., Greiner M. T., Hudson Z. M., Wang S., Liu Z. W., and Lu Z. H. Unlocking the full potential of organic light-emitting diodes on flexible plastic. *Nat Photon*, 5(12):753–757, 12 2011.

[3] Colin M.L. Burnett. File: Artificial neural network.svg, 12 2006. Creative Commons Image [accessed 12-Dec-2011].

[4] Advanced Circuits. Pcb artist. [Free software; accessed 5-Nov-2011].

[5] Jing Feng, Takayuki Okamoto, and Satoshi Kawata. Highly directional emission via coupled surface-plasmon tunneling from electroluminescence in organic light-emitting devices. *Applied Physics Letters*, 87(24):241109, 2005.

[6] Stephen R. Forrest. The path to ubiquitous and low-cost organic electronic appliances on plastic. *Nature*, 428(6986):911–918, 04 2004.

[7] Craig Freudenrich. How oleds work, March 2005. HowStuffWorks permission for educational use [accessed 4-Dec-2011].

[8] J. Goodman. *Introduction to Fourier Optics.* Roberts and Company Publishers, 2005.

[9] A. Graves. *Supervised Sequence Labelling with Recurrent Neural Networks.* Springer Berlin/Heidelberg, 2012.

[10] Soon Moon Jeong, Yoichi Takanishi, Ken Ishikawa, Suzushi Nishimura, Goroh Suzaki, and Hideo Takezoe. Sharply directed emission in microcavity organic light-emitting diodes with a cholesteric liquid crystal film. *Optics Communications*, 273(1):167 – 172, 2007.

[11] A.V. Krishnamoorthy, G. Yayla, and S.C. Esener. Design of a scalable opto-electronic neural system using free-space optical interconnects. In *Neural Networks, 1991., IJCNN-91-Seattle International Joint Conference on*, volume i, pages 527 –534 vol.1, jul 1991.

[12] H. Lamela, M. Ruiz-Llata, and C. Warde. Prototype optoelectronic neural network for artificial vision systems. In *IECON 02 [Industrial Electronics Society, IEEE 2002 28th Annual Conference of the]*, volume 2, pages 1434 – 1438 vol.2, nov. 2002.

[13] R.A. Morgan. Vcsel research, development and applications at honeywell. In *Vertical-Cavity Lasers, Technologies for a Global Information Infrastructure, WDM Components Technology, Advanced Semiconductor Lasers and Applications, Gallium Nitride Materials, Processing, and Devi*, pages 5 –6, aug 1997.

[14] Saito M. Murai R. Sony, panasonic in talks to make oled tvs: sources. [Accessed 20-May-2012].

[15] MIT Department of Chemistry. Module 3: Polymer light emitting devices. Lab handout for class 5.35, sponsored by Timothy M. Swager.

[16] Encyclopedia of Laser Physics and Technology. Bragg mirrors, 2011. [Online; accessed 5-Dec-2011].

[17] Princeton Optronics. Vcsel products. Online vendor [Accessed 20-May-2012].

[18] Corinne E. Packard, Katherine E. Aidala, Sulinya Ramanan, and Vladimir Bulovic. Patterned removal of molecular organic films by diffusion. *Langmuir*, 27(15):9073–9076, 2011.

[19] F.H. Peters, M.G. Peters, D.B. Young, J.W. Scott, B.J. Thibeault, S.W. Corzine, and L.A. Coldren. High-power vertical-cavity surface-emitting lasers. *Electronics Letters*, 29(2):200 –201, jan. 1993.

[20] Takahiro Shiga, Hisayoshi Fujikawa, and Yasunori Taga. Design of multiwavelength resonant cavities for white organic light-emitting diodes. *Journal of Applied Physics*, 93(1):19–22, 2003.

[21] Travis Simpkins, Clifton Fonstad, and Cardinal Warde. Architecture of the compact optoelectronic integrated neural (coin) coprocessor. *AIP Conference Proceedings*, 860(1):113–121, 2006.

[22] Travis L. Simpkins. *Design, Modeling and Simulation of a Compact Optoelectronic Neural Coprocessor.* PhD dissertation, Massachusetts Institute of Technology, Department of Electrical Engineering and Computer Science, 2006.

[23] T. Sotohebo, M. Watanabe, and F. Kobayashi. A compressed implementation of neural network with finite physical quantities on fpgas. In *SICE 2002. Proceedings of the 41st SICE Annual Conference*, volume 3, pages 1861 – 1862 vol.3, aug. 2002.

[24] Tetsuo Tsutsui, Noriyuki Takada, Shogo Saito, and Etsuo Ogino. Sharply directed emission in organic electroluminescent diodes with an optical-microcavity structure. *Applied Physics Letters*, 65(15):1868–1870, 1994.

[25] Peter Vandersteegen, Saso Mladenovski, Volker van Elsbergen, Georg Gartner, Peter Bienstman, Kristiaan Neyts, and Roel Baets. Light extraction for a doubly resonant cavity organic led: the rc[sup 2]led. volume 6655, page 665513. SPIE, 2007.

[26] C. Warde. Compact optoelectronic signal processors. In *LEOS '99. IEEE Lasers and Electro-Optics Society 1999 12th Annual Meeting*, volume 1, pages 325 –326 vol.1, 1999.